EARTHQUAKE ENGINEERING AND STRUCTURAL DYNAMICS, VOL. 25, 371–400 (1996)

PREDICTION OF HORIZONTAL RESPONSE SPECTRA IN EUROPE

N. N. AMBRASEYS*, K. A. SIMPSON† AND J. J. BOMMER‡

Civil Engineering Department, Imperial College of Science Technology and Medicine, London SW7 2BU, U.K.

SUMMARY

A large and uniform dataset is used to find equations for the prediction of absolute spectral acceleration ordinates in Europe and adjacent areas, in terms of magnitude, source-distance and site geology. The dataset used is shown to be representative of European strong motion in terms of the attenuation of peak ground acceleration. The equations are recommended for use in the range of magnitudes from M_S 4·0 to 7·5 and for source-distances of up to 200 km.

KEY WORDS: strong-motion; attenuation; horizontal response spectra; Europe; site effects; seismic design

INTRODUCTION

Scope of study

The objective of this study is to provide relationships which can be used in the construction of hazard-consistent design spectra in Europe and the Middle East. In normal earthquake-resistant engineering design the seismic loads are represented by response spectra. A common approach for obtaining a design spectrum is to perform a hazard analysis in terms of parameters such as peak ground acceleration and then anchor a standard spectral shape to the design value of zero-period acceleration; this is the methodology adopted in Eurocode 8. McGuire[1] showed that this approach often results in spectra which do not represent the same hazard level at all periods. In order to overcome this inconsistency, McGuire[1] proposed carrying out seismic hazard analysis in terms of spectral ordinates at different periods, using frequency-dependent attenuation equations as originally proposed by Johnson.[2]

So far the majority of published studies for different parts of the world have used pseudo-relative velocity spectra as the response variable in frequency-dependent attenuation equations.[3–8] Pseudo-response spectra were originally adopted when computer technology was such that the generation of spectral ordinates was time consuming and expensive and thus it was convenient to determine only the relative displacement response and use this to estimate the relative velocity and absolute acceleration response.[9] Today the generation of response spectra is trivial in terms of computer effort and we are unsure why the pseudo-spectra continue to be used so widely, except perhaps that their use makes it easy to compare results with previous equations and with other spectrum construction techniques which have also been based on the tripartite representation.[10,11]

Since in current design practice the engineer uses the absolute acceleration response, even the advantage of being able to represent the three spectra simultaneously on a single plot is unclear in view of the difficulty of reading values from an inclined and crammed logarithmic scale. For these reasons we have opted instead to use the absolute acceleration response as the dependent variable in our equations, as has been done in a few previous studies, such as Kawashima *et al.*[12]

* Senior Research Fellow
† Research Associate
‡ Lecturer

CCC 0098–8847/96/040371–30

Received 17 June 1995
Revised 25 October 1996

In this study the larger horizontal acceleration response ordinate for 5 per cent of critical damping at each period was taken from each triaxial record. The response variable, therefore, is the envelope of the two horizontal spectra from each recording. The larger value of peak horizontal ground acceleration was also used in order to fix the zero-period level of the spectrum.

Previous studies

Frequency-dependent relationships for spectral ordinates have been derived for many parts of the world, particularly for the United States and Japan, several of which are reviewed by Joyner and Boore.[13]

For the European area, there are two published studies of spectral attenuation, presented by Mohammadioun[14] for Italian data and by Petrovski and Marcellini[5] for the Eastern Mediterranean region, the more seismically active part of the continent. The Mohammadioun study uses 288 components from 144 triaxial records generated by 49 events to determine pseudo-velocity response ordinates for frequencies from 0·513 to 78·0 Hz. Site geology is not included in the attenuation model. Mohammadioun stresses that the results are only preliminary, principally due to the use of focal distances rather than more appropriate fault distances.

In the Petrovski and Marcellini[5] study, equations were derived for pseudo-velocity response ordinates in the period range 0·02 to 5·0 s, using for the regression analysis 120 triaxial strong-motion records generated by 46 earthquakes, of which 23 were from former Yugoslavia, 20 from northern Italy and 3 from northern Greece; the Friuli and Montenegro earthquakes of 1976 and 1979 generated 93 of the 120 records in their dataset. The geometric attenuation term in their model included arbitrary constant values added to the focal distance term to simulate near-field effects, and the site geology was not considered.

Elsewhere, European records have been incorporated into world-wide datasets, such as Dahle *et al.*[6] The purpose of this paper is to present the results from an investigation of the attenuation with distance of spectral ordinates in the active part of the European and Middle Eastern area.

DATA

The dataset used in this study to derive response spectra attenuation equations consists of 422 triaxial records available to us generated by 157 earthquakes in Europe and adjacent regions, with surface wave magnitude M_S between 4·0 and 7·9 and focal depth less than or equal to 30 km. The lower limit on magnitude was chosen because smaller earthquakes are generally not of engineering significance. The strong-motion recordings used in this study have been extracted from the European databank which has been presented previously,[15,16] and subsequently updated.

In this dataset, the predictor variables (the focal depth and magnitude for each earthquake, the site geology for each recording station and the source-site distance for each record) were reviewed and most of them re-evaluated. This revision was considered to be necessary since the data come from a variety of sources of different accuracy and reliability. The dataset is presented in the appendix.

Source distance

The assessment of source distance requires accurate source locations as well as reliable station positions. A comparison of the position of strong-motion instruments reported by a number of national agencies with those re-determined in this study using large-scale maps or, on request, by the owners of the instrument, showed differences in location of up to 10 km.

As the source distance we adopted the closest distance to the projection of the fault rupture, as defined by Joyner and Boore.[17] For most of the larger earthquakes ($M_S > 6·0$) in our dataset we have adequate data to estimate with acceptable accuracy source distances of strong-motion stations. For small magnitude crustal earthquakes the source distance is close to the epicentral distance, with an uncertainty not normally larger than that associated with the determination of the epicentre. However, the locations of some of the smaller events are poorly known. For this reason some of the epicentral locations were re-evaluated which allowed the adoption of improved positions. Nevertheless, given the uncertainties in relocation procedures differences in position of up to about 10 km are very likely with no foreseeable means of improving them.

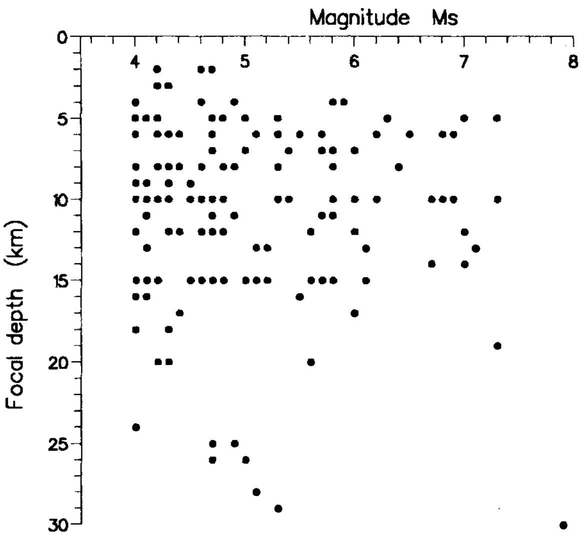

Figure 1. Distribution of the earthquakes in the dataset in terms of magnitude and revised focal depth

Focal depth

In our re-examination of locations, the least well-determined parameter is depth. In order to set an approximate minimum hypocentral distance we used the interval between the triggering time and the first S-wave arrivals (S_t) read from true-to-scale copies of the original analogue traces. For many of the strong-motion records it was possible for S_t to be estimated from one or more components of motion and be used to assess focal distance, by employing a number of crustal velocity profiles for the Eastern Mediterranean region obtained from special studies.

Figure 1 shows the distribution of earthquakes in the dataset with respect to their revised focal depth; the majority of them (81 percent) are in the range of h, 5–15 km.

Local soil conditions

The information in our dataset concerning depths of soil deposits and soil properties, shear wave velocity V_S, cone and standard penetration test profiles is incomplete. It has nonetheless been possible to classify 207 of the 212 permanent and temporary strong-motion stations in our dataset into four categories. These categories are similar to those used by Boore *et al.*,[7] based on shear wave velocities, V_S, averaged over the upper 30 m of the site. The classes of site geology are defined by the following ranges of average V_S: rock (R) > 750 m/s; stiff soil (A) 360–750 m/s; soft soil (S) 180–360 m/s, and very soft soil (L) < 180 m/s. For 53 sites we do have detailed local soil and velocity profiles but for the other sites the conditions are known in terms of only the most general classification. The site conditions for 416 of the 422 records in the dataset have been classified and there are 106, 226, 81 and 3 records in the (R), (A), (S) and (L) categories respectively.

Magnitudes

We avoided using the local magnitude because there are no M_L determinations for earthquakes in some parts of the study area (Algeria, Iran, Turkey and the former USSR) and also because average estimates ofM_L in our study area come from very few stations and they are not always reliable due to the different calibration methods used.

The use of a size estimate in terms of seismic moment is also not possible since only one-third of the earthquakes in our dataset have a M_0 value available from Harvard centroid moment tensor determinations or from special studies.

These restrictions justify our choice of M_S for all magnitudes rather than the adoption of the hybrid use of M_L and M_S employed in some attenuation laws for western North American earthquakes (e.g. Reference 18) and subsequently adopted in other regions as well.[19,20] For magnitudes less than 6·0, the U.S. practice, in contrast with Europe, is to use M_L instead of M_S. Moreover, M_S is the best estimator of the size of a crustal earthquake, not only because of the large number of teleseismic data that are available for its assessment but also because of its excellent correlation with seismic moment M_0. In addition to these considerations, since seismicity in the European area is generally evaluated in terms of M_S it is necessary to use the same scale in the attenuation relation in order to use the equation in hazard analysis.

Surface wave magnitudes M_S were calculated, therefore, for all events in the dataset using the Prague formula,[21] with a period restriction which is distance dependent,[22] and for close seismograph stations with amplitudes and periods of the L_g phase. We have assumed an average crustal thickness for our region of 30 km which we set as the lowest limit for the validity of the application of the Prague formula, beyond which M_S values need correction for depth. For a few smaller events it was not possible to obtain sufficient seismogram readings, so M_S values were obtained by conversion from other magnitude scales.

Moment magnitude

The standard definition of moment magnitude **M** of Hanks and Kanamori[23] widely used today in the derivation of attenuation laws is

$$\mathbf{M} = (2/3)\log(M_0) - 10{\cdot}7 \qquad (1)$$

a linear relation in **M** and $\log(M_0)$, in which M_0 is the calculated seismic moment in dyn cm. Moment magnitude **M** is considered by Hanks and Kanamori[23] to be equivalent to M_S in the range $5 \leqslant M_S \leqslant 7\frac{1}{2}$ (and equivalent to M_L and M_W over the ranges $3 \leqslant M_L \leqslant 7$ and $M_W \geqslant 7\frac{1}{2}$, respectively). With regard to the magnitude M_W of Kanamori,[24] some confusion has arisen in the literature with M_W often referred to as the moment magnitude (e.g. References 25 and 26) and assigned to earthquakes of all sizes, whereas Kanamori[24] only considers great earthquakes, the smallest value of M_W in his dataset being 7·2.

A regression for which M_0, recalculated M_S values and focal depths are available for 700 earthquakes from Europe, using a dichotomous quadratic polynomial with depth correction, gives:

$$M_S = -48{\cdot}443 + 3{\cdot}487[\log(M_0)] - 0{\cdot}05266[\log(M_0)]^2 - 0{\cdot}0036(h - 30)p \qquad (2)$$

with a standard deviation of only 0·23. In equation (2), which is valid for $23{\cdot}8 \leqslant \log(M_0) \leqslant 27{\cdot}8$, p is 0 for a focal depth $h \leqslant 30$ and 1 for $h > 30$ km.

Figure 2 with equation (2) plotted for $p = 0$ shows that for M_S magnitudes smaller than about 6·0, the observed $M_S - \log(M_0)$ relation departs from that proposed by Hanks and Kanamori[23] and that with decreasing moment below about $1{\cdot}0 \times 10^{25}$ dyn cm the difference between M_S and **M** increases, becoming 0·5 of a magnitude unit for $6{\cdot}0 \times 10^{23}$ dyn cm ($\mathbf{M} \approx 5$). In other words, this plot confirms, as it should, that for small events M_S and $\log(M_0)$ have a 1:1 relation. For intermediate magnitudes, however, the ratio is 1:1·5, and it reaches 1:2 for very large events.

This behaviour of small events is confirmed from a larger body of data in our files from the Eastern Mediterranean region, Central America and Iran and is also consistent with the global average relation of Ekström and Dziewonski[25] which is shown in Figure 2 for comparison. A consequence of this is that for surface wave magnitudes of less than about 6·0, M_S and **M** are not interchangeable, and that in an attenuation law, a linear scaling with magnitude M_S would be a non-linear scaling if **M** were used. This is an important consideration for our dataset and for other datasets obtained in areas of low seismicity such as north-western Europe, dominated by relatively small magnitude events, and precludes the joint use of **M** as defined by equation (1) and M_S as size estimators in datasets with events smaller than about M_S 6·0.

Strong-motion records

Most of our accelerograms come chiefly from analogue SMA-1 type instruments, with a few from MO-2, AR-240, MR2002, SSA-1, SM1, ASZ-2 and SRZ instruments.

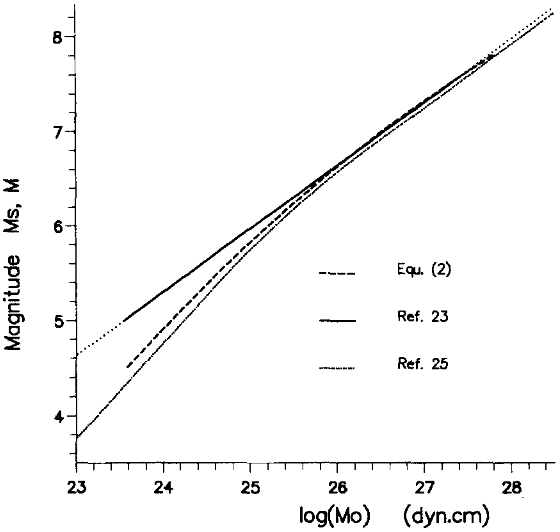

Figure 2. Comparison of the M_S-log(M_0) relationship for shallow focus ($h \leqslant 30$ km) earthquakes from this study (equation (2)), with the moment magnitude relationship of Hanks and Kanamori[23] (equation (1)) and the M_S-log(M_0) relationship of Ekström and Dziewonski[25]

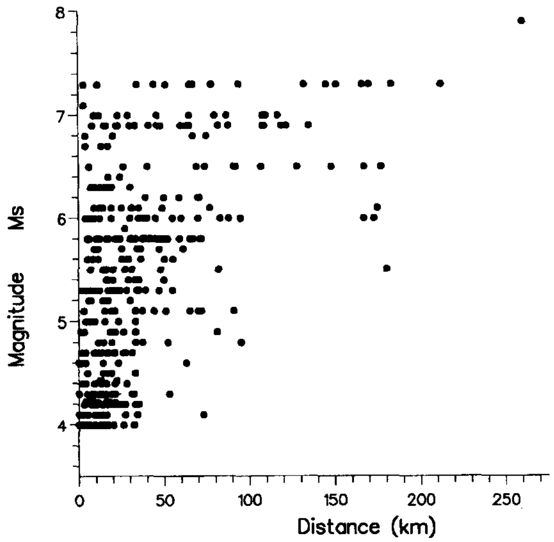

Figure 3. Distribution of the dataset with respect to magnitude M_S and distance

Most of the records come from free-field stations although some are from basements or ground floors of relatively small structures, and tunnel portals. We have not excluded records obtained at distances greater than the shortest distance to a reportedly operational but non-triggered instrument. The reasons for this are that the trigger levels for different types of instruments in use in our area are not constant or may not be known. For example, during recording of the Friuli (Italy) sequence in 1976,[27] we know that the trigger threshold on some of the SMA-1 instruments was set much lower than the normal 0·01 g specification. Furthermore, it is not always possible to know whether non-triggering was genuinely due to the low value of ground motion or because of malfunction of the instrument.

Figure 3 shows the distribution of our dataset with respect to M_S and source-site distance, from which it can be seen that the data covers reasonably the range of M_S from 4·0 to 7·5 and distances up to 200 km from the earthquake source.

Preprocessing of records

All European acceleration records available to us and satisfying the previously defined criteria were plotted, together with their integrated velocity and displacement time-histories, and visually inspected. Those records showing anomalies were treated individually in order to remove errors at source wherever possible, although the digitization quality of several accelerograms was judged to be sufficiently poor to justify their exclusion from the dataset. The recoverable errors were mainly spurious points in the digitized data and translations and rotations of the baseline for all or part of the record. The spurious points were simply eliminated from the record in those cases where their nature was obvious or could be confirmed by comparison with copies of the original analogue traces.

Baseline translations and rotations were corrected by linear least-squares fitting over the intervals before and after the shift, and then the two parts were spliced to obtain a smooth record and align the baseline.

In those cases where more than one digitized version of a particular accelerogram existed, the selected record was chosen on the basis of the quality of the digitization, where the difference was clear from inspection. Otherwise the selection was made on the basis of greater duration, except for those cases where the duration were comparable, whence the record having the smaller average sampling interval was chosen.

Correction procedures

Once the pre-processing had been performed, a uniform correction procedure was applied to all the records in order to reduce noise in the high- and low-frequency ranges. No correction was applied for the instrument characteristics because reliable values of the natural frequency and damping of the accelerometer transducers are not available for a large proportion of the records. For standard accelerographs such as the SMA-1, which represent the bulk of the instruments that recorded our dataset, the instrument characteristics only significantly distort the recorded amplitude at frequencies higher than about 25 Hz and since the smallest response period considered in this study is 0·1 s, the contamination is not important.

The correction procedure applied to each record depended upon the total digitized duration. For very short time histories with duration not exceeding 5 s, a parabolic baseline adjustment was made using a least-squares fitting.

For records with durations greater than 10 s, the data was resampled at a constant time interval of 0·01 s and an elliptical filter was applied, using a programme developed by Menu[28] based on the filter design proposed by Shyam Sunder and Connor;[29] the limits of the filter pass band were 0·20 and 25·0 Hz.

For those records having durations between 5 and 10 s, both the polynomial baseline and the filtering procedures were applied and the more effective correction selected on the basis of the appearance of the adjusted time histories and realistic values of the maximum ground displacement.

RESULTS

Attenuation of peak ground acceleration

In an earlier paper, equations for the prediction of peak accelerations in Europe were derived from a dataset of 529 recordings.[30] A subsequent paper presented new equations, based on an extended dataset with a total of 1260 records from Europe and adjacent areas,[31] which were almost identical. In this study, in order to obtain equations which are consistent with those for the prediction of spectral ordinates, the smaller set of 422 triaxial recordings, those for which spectra are available, has been used.

The attenuation model used initially includes only magnitude and distance as independent variables. Linear magnitude scaling and a magnitude-independent shape are adopted and both anelastic and geometric distance terms included, the general form of the equation being:

$$\log(y) = C_1 + C_2 M + C_3 r + C_4 \log(r) + \sigma P \tag{3}$$

where y is the parameter being predicted, in this case peak horizontal ground acceleration in g, M_S is the surface wave magnitude, and:

$$r = \sqrt{d^2 + h_0^2} \tag{4}$$

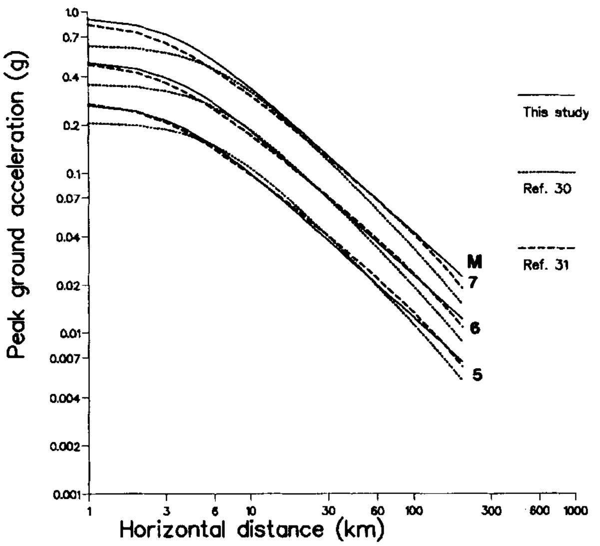

Figure 4. Comparison of values of peak horizontal ground acceleration predicted for magnitudes of 5, 6 and 7 and different source-site distances by equations (5), (7) and (8)

where d is the shortest distance from the station to the surface projection of the fault rupture, in km, and h_0 is a constant to be determined with C_1, C_2, C_3 and C_4. The standard deviation of $\log(y)$ is σ, and the constant P takes a value of 0 for mean values and 1 for 84-percentile values of $\log(y)$.

The term h_0 in equation (4) accounts for the fact that the source of the peak motion is not necessarily the closest point on the surface projection of the fault, or from the epicentre, and it does not represent explicitly the effect of the depth on the acceleration.

In this study we have chosen to employ the two-state regression technique[32] originally proposed by Joyner and Boore[17] to decouple the determination of distance dependence from the determination of magnitude dependence.

It is found that the distribution of the dataset is not sufficiently large to determine simultaneously both the anelastic (C_3) and geometric attenuation (C_4) coefficients, since a positive value of C_3 is obtained. The analysis was therefore performed constraining C_3 to zero since the influence of the anelastic attenuation in the near-field is relatively small, and the following equation was obtained:

$$\log(a) = -1{\cdot}39 + 0{\cdot}266M_S - 0{\cdot}922\log(r) + 0{\cdot}25P \tag{5}$$

with $h_0 = 3{\cdot}5$. The analysis was also performed using a direct one-stage regression, and a small but permissible value of C_3 was found:

$$\log(a) = -1{\cdot}52 + 0{\cdot}261M_S - 0{\cdot}00045(r) - 0{\cdot}815\log(r) + 0{\cdot}25P \tag{6}$$

where $h_0 = 1{\cdot}9$. Equations (5) and (6) predict almost identical values of acceleration over the range of distances which are of engineering interest.

Figure 4 shows a plot of equation (5) for magnitudes 5·0, 6·0 and 7·0. Also shown for comparison are plots of the equations for peak horizontal acceleration for $M_S \geqslant 4{\cdot}0$ obtained by Ambraseys and Bommer:[30]

$$\log(a) = -1{\cdot}09 + 0{\cdot}238M_S - 0{\cdot}00050(r) - \log(r) + 0{\cdot}28P \tag{7}$$

with $h_0 = 6{\cdot}0$, and by Ambraseys:[31]

$$\log(a) = -1{\cdot}43 + 0{\cdot}245M_S - 0{\cdot}0010(r) - 0{\cdot}786\log(r) + 0{\cdot}24P \tag{8}$$

with $h_0 = 2{\cdot}7$.

From Figure 4 it is interesting to note that although the datasets were not the same and the number of data points used in these three derivations were 422, 529 and 1260, there is little difference between the results of the regressions; in the range of distances from 5 to 50 km, they are almost identical. The differences between the accelerations predicted by equations (5), (7) and (8) are a small fraction of the individual standard deviations, which have also changed very little. It would appear from this, therefore, that equation (5) and the reduced dataset to be used for spectral ordinate attenuation is representative of the behaviour of European earthquakes.

Inclusion of the site geology in the attenuation model

Although the conditions under which site geology may amplify or de-amplify peak ground motion have not been conclusively established, it is clear that local site geology plays an important role in influencing both the shape and amplitude of the response spectrum.

There are only three records in our dataset recorded on very soft (L) soil. Obviously, these records cannot be considered in a separate category as they would give undue weighting to particular topographical and stratigraphical conditions. However, rather than omit these records, which may be as typical as any other, we have chosen initially to include them in the soft soil (S) category. A subsequent examination of the residuals of the regression solution which includes site geology would reveal if these three very soft records occur as 'outliers' and therefore suggest their inclusion in the soft soil category may be inappropriate.

Figure 5 shows the distribution in magnitude-distance space of the records in each site category. It can be seen that the distributions are reasonably uniform with each category represented by a comparable number of data points.

The method that we have chosen to apply for the regression analysis follows the same logic as the two-stage procedure which is designed to decouple the determination of magnitude and distance dependence. Having performed the two-stage regression, the residuals, ε_i, are calculated for each record from equation (3):

$$\varepsilon_i = \log(y_i) - C_1 - C_2 M_j - C_4 \log(r_i) \tag{9}$$

where r_i is the source-site distance for the ith record, generated by the jth earthquake. The regression is then performed on the following equation:

$$\varepsilon = C_5 S_R + C_6 S_A + C_7 S_S \tag{10}$$

where S_R takes the value of 1 if the site is classified as rock (R) and 0 otherwise, and S_A and S_S are similarly defined for stiff (A) and soft (S) soil sites. Equation (3) is then modified (taking into account that the coefficient C_3 has been constrained to zero) to become

$$\log(y) = C_1' + C_2 M + C_4 \log(r) + C_A S_A + C_S S_S + \sigma P \tag{11}$$

in which the new coefficients are defined as follows:

$$C_1' = C_1 + C_5 \tag{12}$$

$$C_A = C_6 - C_5 \tag{13}$$

$$C_S = C_7 - C_5 \tag{14}$$

and the error term σ is re-calculated using the residuals with respect to the site-dependent prediction. Applying this procedure, the regression on equation (10) was performed using the residuals with respect to equation (5) for the 416 records for which site conditions have been classified, and the following equation was obtained:

$$\log(a) = -1{\cdot}48 + 0{\cdot}266 M_S - 0{\cdot}922 \log(r) + 0{\cdot}117 S_A + 0{\cdot}124 S_S + 0{\cdot}25 P \tag{15}$$

with the value of h_0 still being 3·5. The equation shows that expected values of peak horizontal ground acceleration will be about 32 per cent larger on any soil site than on rock, but the inclusion of this term has not significantly reduced the scatter. In our previous studies,[30,31] we have demonstrated that the site-

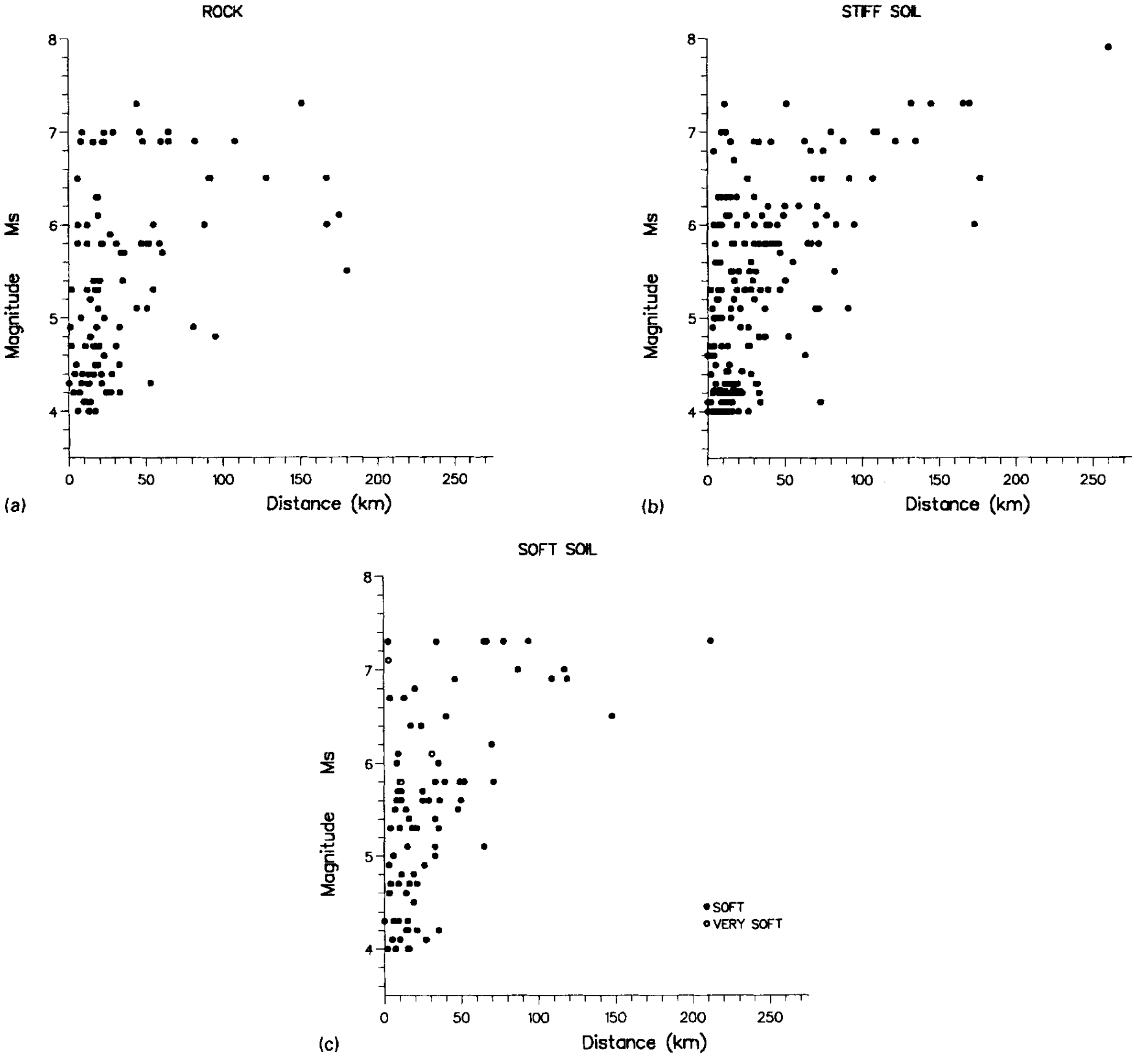

Figure 5. Distribution in magnitude-distance space of the data subsets grouped according to the site geology: (a) rock, (b) stiff soil, (c) soft soil and very soft soil

independent predictive equations for the European area are very similar to those derived for western North America,[17] and here we make a similar comparison with the site-dependent equation produced by Boore *et al.*[7] for the larger component of peak horizontal acceleration:

$$\log(a) = -1{\cdot}334 + 0{\cdot}216M - 0{\cdot}777\log(r) + 0{\cdot}158G_B + 0{\cdot}254G_C + 0{\cdot}21P \tag{16}$$

where r is defined as in equation (4) with $h_0 = 5{\cdot}48$, and where G_B and G_C are variables which are equivalent to the variables S_A and S_S in equation (15); their class D, which is equivalent to our very soft (L) classification, was considered to be poorly represented in their dataset and was simply ignored rather than incorporated into their class C, equivalent to our soft (S) site classification.

Direct comparison between the European and North American equations is complicated by the fact that Boore *et al.*[7] have used **M** to measure earthquake size. In Figures 6 and 7 we compare the predicted values of

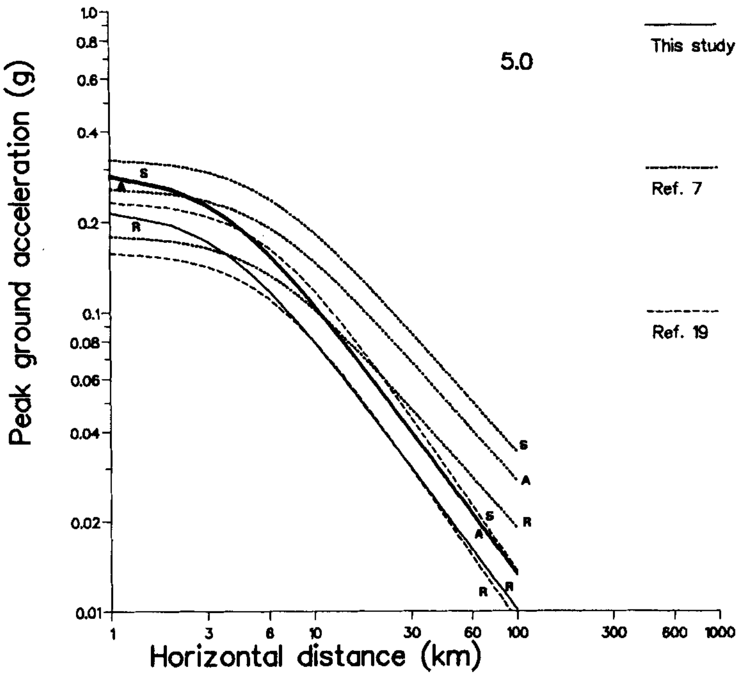

Figure 6. Predicted values of peak horizontal acceleration as a function of distance for an earthquake of magnitude M_S 5, according to equations (15) and (16), for rock, stiff and soft soil sites, and according to the equation of Sabetta and Pugliese[19] for rock and soil sites

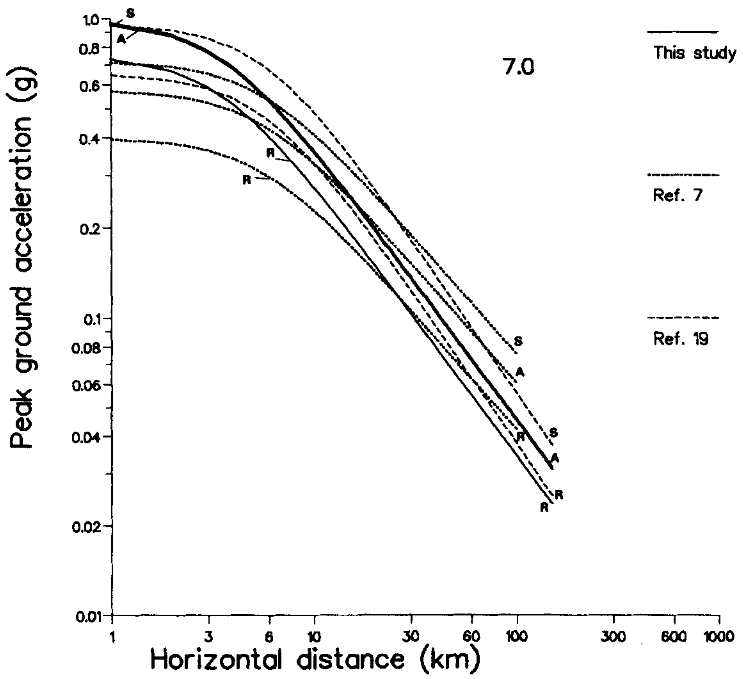

Figure 7. Predicted values of peak horizontal acceleration as a function of distance for an earthquake of magnitude M_S 7, according to equations (15) and (16), for rock, stiff and soft soil sites, and according to the equation of Sabetta and Pugliese[19] for rock and soil sites

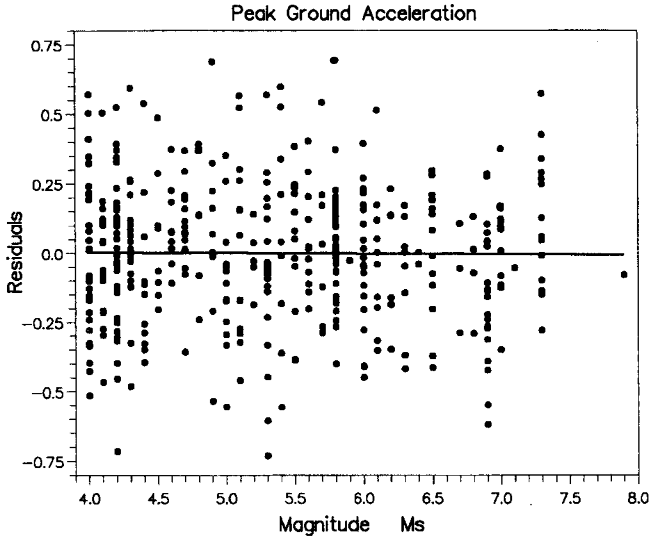

Figure 8. Residuals of the logarithm of peak acceleration from equation (15) as a function of magnitude

horizontal acceleration at different distances for events of magnitude M_S 5·0 and 7·0, respectively, for rock, stiff and soft soil sites, using equations (15) and (16); in the second equation **M** values of 5·4 and 6·9 are used, converted from M_S to $\log(M_0)$ through an equation similar to equation (2) but found by regressing $\log(M_0)$ on M_S, then to **M** through equation (1). In this way, the magnitude value used in both equations corresponds to the same seismic moment.

In Figures 6 and 7 the accelerations are also compared with those predicted by the equations of Sabetta and Pugliese[19] for Italian earthquakes. These equations include a dichotomous term for the site geology, where 'soil' includes only shallow sites where the deposits are between 5 and 20 m thick and have shear wave velocities of 400 to 800 m/s, and 'rock' includes stiff sites (having shear wave velocities in excess of 800 m/s), with or without a thin (< 5 m) soil (V_S 400–800 m/s) layer, and deep soil sites (deposits with shear wave velocities between 400 and 800 m/s, greater than 20 m deep).

It should be pointed out that the regression method used by us differs from that of Boore *et al.*,[7] who use a two-stage solution with the soil coefficients determined with the distance term in the first part of the regression. Our method is also different from that of Sabetta and Pugliese,[19] who use a one-stage solution. We have tested these two methods on our dataset, together with a fourth method in which the magnitude and distance terms are derived from a one- or two-stage regression performed solely on the rock records of the dataset, and the soil coefficients are then determined from the residuals of all the records with respect to this rock only equation. We have also performed regressions using the various methods on our dataset in which records from equal magnitude events were grouped together because our dataset has many poorly recorded earthquakes. This magnitude grouping reduced the number of separate 'events' from 157 to 33. The different regressions produced results which were mostly similar, although in a few cases marked differences occurred: for example, using the two-stage approach of Boore *et al.*[7] the soil coefficients in equation (15) were dramatically reduced, the stiff soil term to 0·05 and the soft soil term to 0·02. Each of the regression methods used has limitations, a problem we are currently considering, and there is no 'best' method, different approaches being more appropriate for different datasets.

Residual plots of equation (15) for the full dataset as functions of magnitude and distance are shown in Figures 8 and 9 together with linear best-fit relations. With respect to magnitude no significant trends are observed for the full dataset, nor for any of the site categories. For distance, apparent linear trends are found (Figure 10), particularly for the rock dataset; however F-tests reveal a significant lack of fit of the regression at the 95 per cent confidence level. It is noted that the gradients in the residual-distance plots for rock and stiff

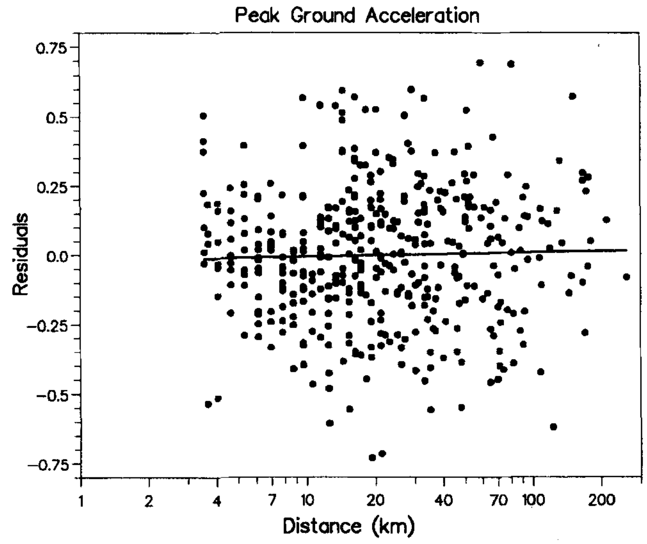

Figure 9. Residuals of the logarithm of peak acceleration from equation (15) as a function of distance

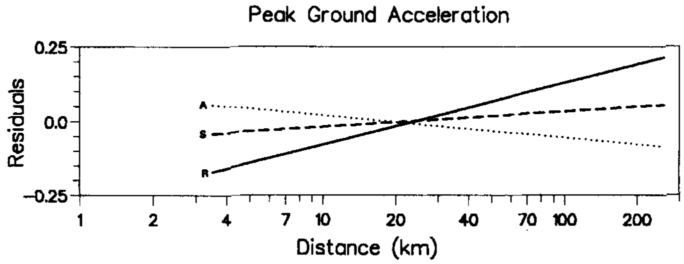

Figure 10. Regressions of residuals of logarithms of peak acceleration on distance for three different site categories

soil have opposite sign, implying that the actual difference between them may be more significant. This can be tested by examining the residuals from the regression solution derived using only the rock data for the magnitude and distance coefficients described above. F-tests on these residuals reveal for both stiff and soft soil groups a significant, and in the case of the stiff group, a useful regression at the 95 per cent level, where useful is a F-value 10 times the F-critical. This suggests that distance dependency could be incorporated into the soil coefficients to improve the model were this regression approach adopted.

Attenuation of spectral ordinates

Regression analysis, using a two-stage procedure, was applied to the absolute acceleration spectral ordinates in g, of the same 422 records used to derive equation (5). In this analysis we used linear magnitude scaling and a magnitude-independent shape, employing the attenuation model in the equation (3). The spectral ordinates, damped at 5 per cent critical, cover the range between 0·1 and 2·0 s, at the same intervals set out by the CALTECH volumes.[33] The regressions were first performed allowing both C_3 and C_4 to be determined simultaneously, but inadmissible values of the anelastic coefficient were obtained for short periods from 0·10 to 0·24 s and in some higher period ranges, from 0·60 to 0·70 and 0·95 to 1·80 s. For this reason, in all cases the C_3 term in equation (3) was constrained to zero, although the equations found either way predict almost identical values of acceleration at distances of less than 200 km.

The results from the two-stage regression were then used to determine the coefficients of the site-dependent terms in equation (11), using the 416 records with site classification, and the results are listed, without

Table I. Coefficients of equation (11) for spectral ordinates

T	C'_1	C_2	h_0	C_4	C_A	C_S	σ
0·10	− 0·84	0·219	4·5	− 0·954	0·078	0·027	0·27
0·11	− 0·86	0·221	4·5	− 0·945	0·098	0·036	0·27
0·12	− 0·87	0·231	4·7	− 0·960	0·111	0·052	0·27
0·13	− 0·87	0·238	5·3	− 0·981	0·131	0·068	0·27
0·14	− 0·94	0·244	4·9	− 0·955	0·136	0·077	0·27
0·15	− 0·98	0·247	4·7	− 0·938	0·143	0·085	0·27
0·16	− 1·05	0·252	4·4	− 0·907	0·152	0·101	0·27
0·17	− 1·08	0·258	4·3	− 0·896	0·140	0·102	0·27
0·18	− 1·13	0·268	4·0	− 0·901	0·129	0·107	0·27
0·19	− 1·19	0·278	3·9	− 0·907	0·133	0·130	0·28
0·20	− 1·21	0·284	4·2	− 0·922	0·135	0·142	0·27
0·22	− 1·28	0·295	4·1	− 0·911	0·120	0·143	0·28
0·24	− 1·37	0·308	3·9	− 0·916	0·124	0·155	0·28
0·26	− 1·40	0·318	4·3	− 0·942	0·134	0·163	0·28
0·28	− 1·46	0·326	4·4	− 0·946	0·134	0·158	0·29
0·30	− 1·55	0·338	4·2	− 0·933	0·133	0·148	0·30
0·32	− 1·63	0·349	4·2	− 0·932	0·125	0·161	0·31
0·34	− 1·65	0·351	4·4	− 0·939	0·118	0·163	0·31
0·36	− 1·69	0·354	4·5	− 0·936	0·124	0·160	0·31
0·38	− 1·82	0·364	3·9	− 0·900	0·132	0·164	0·31
0·40	− 1·94	0·377	3·6	− 0·888	0·139	0·172	0·31
0·42	− 1·99	0·384	3·7	− 0·897	0·147	0·180	0·32
0·44	− 2·05	0·393	3·9	− 0·908	0·153	0·187	0·32
0·46	− 2·11	0·401	3·7	− 0·911	0·149	0·191	0·32
0·48	− 2·17	0·410	3·5	− 0·920	0·150	0·197	0·32
0·50	− 2·25	0·420	3·3	− 0·913	0·147	0·201	0·32
0·55	− 2·38	0·434	3·1	− 0·911	0·134	0·203	0·32
0·60	− 2·49	0·438	2·5	− 0·881	0·124	0·212	0·32
0·65	− 2·58	0·451	2·8	− 0·901	0·122	0·215	0·32
0·70	− 2·67	0·463	3·1	− 0·914	0·116	0·214	0·33
0·75	− 2·75	0·477	3·5	− 0·942	0·113	0·212	0·32
0·80	− 2·86	0·485	3·7	− 0·925	0·127	0·218	0·32
0·85	− 2·93	0·492	3·9	− 0·920	0·124	0·218	0·32
0·90	− 3·03	0·502	4·0	− 0·920	0·124	0·225	0·32
0·95	− 3·10	0·503	4·0	− 0·892	0·121	0·217	0·32
1·00	− 3·17	0·508	4·3	− 0·885	0·128	0·219	0·32
1·10	− 3·30	0·513	4·0	− 0·857	0·123	0·206	0·32
1·20	− 3·38	0·513	3·6	− 0·851	0·128	0·214	0·31
1·30	− 3·43	0·514	3·6	− 0·848	0·115	0·200	0·31
1·40	− 3·52	0·522	3·4	− 0·839	0·109	0·197	0·31
1·50	− 3·61	0·524	3·0	− 0·817	0·109	0·204	0·31
1·60	− 3·68	0·520	2·5	− 0·781	0·108	0·206	0·31
1·70	− 3·74	0·517	2·5	− 0·759	0·105	0·206	0·31
1·80	− 3·79	0·514	2·4	− 0·730	0·104	0·204	0·32
1·90	− 3·80	0·508	2·8	− 0·724	0·103	0·194	0·32
2·00	− 3·79	0·503	3·2	− 0·728	0·101	0·182	0·32

smoothing, in Table I. We have chosen not to perform any smoothing of the coefficients because this means introducing arbitrary decisions as to how this should be performed. If smoothing were to be applied it should be with respect to the period T, but if the results were to be converted by any user to psuedo-spectra to present on a tripartite plot, better results would be obtained by smoothing with respect to $\log(T)$.

As for peak acceleration, an examination of residuals for the full dataset and for each site category with respect to magnitude and distance was performed. The residual plots together with their linear best-fit

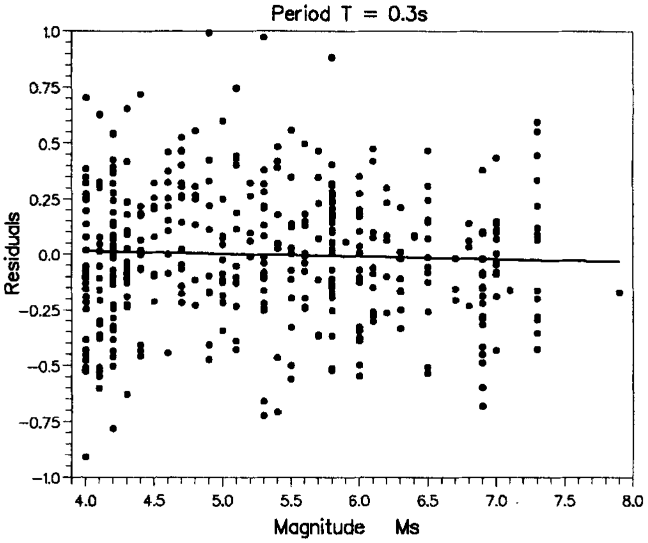

Figure 11. Residuals of the logarithm of spectral acceleration at $T = 0{\cdot}3$ s from equation (11) as a function of magnitude

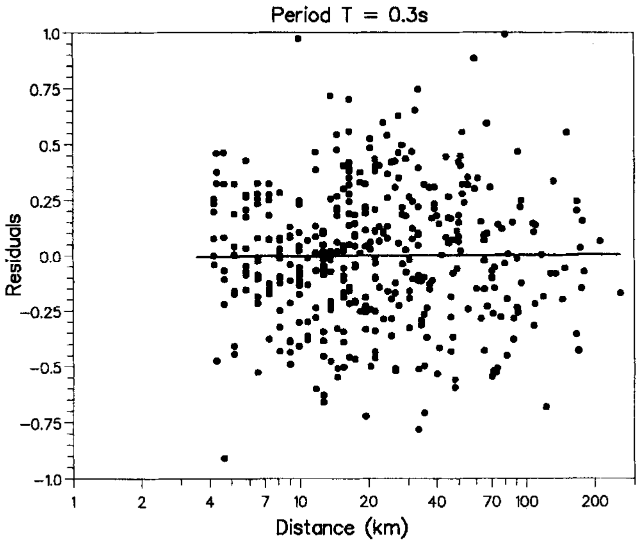

Figure 12. Residuals of the logarithm of spectral acceleration at $T = 0{\cdot}3$ s from equation (11) as a function of distance

relations for periods $T = 0{\cdot}3$ s and $T = 1{\cdot}0$ s are shown in Figures 11–16. Apparent trends are observed with respect to distance in several cases, but F-tests again reveal these proposed linear relations to have a significant lack of fit to the residual data at the 95 per cent confidence level, and hence no modification of the attenuation model was made.

A direct comparison of our results with existing spectral relations is made difficult for two reasons: we have chosen to use absolute acceleration (SA) rather than pseudo-velocity (PSV) usually employed by others, and we use M_S magnitudes exclusively rather than moment $\mathbf{M}$ or hybrid M_L, M_S and $\mathbf{M}$ magnitudes. As for peak ground acceleration, we use the equations of Boore *et al.*[7] for comparison, converting M_S values to $\mathbf{M}$ as done previously, and values of PSV are converted to PSA at each period T via the relation $\mathrm{PSA} = \mathrm{PSV}(2\pi/T)$. Figures 17–19 compare the spectra predicted for different site geologies for three different design scenarios by our equations for Europe and those for western North America.

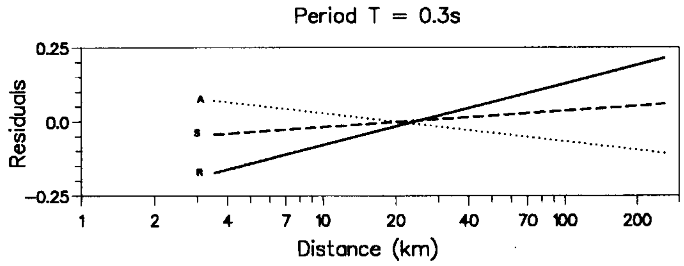

Figure 13. Regressions of residuals of logarithms of spectral acceleration at $T = 0{\cdot}3$ s on distance for three different site categories

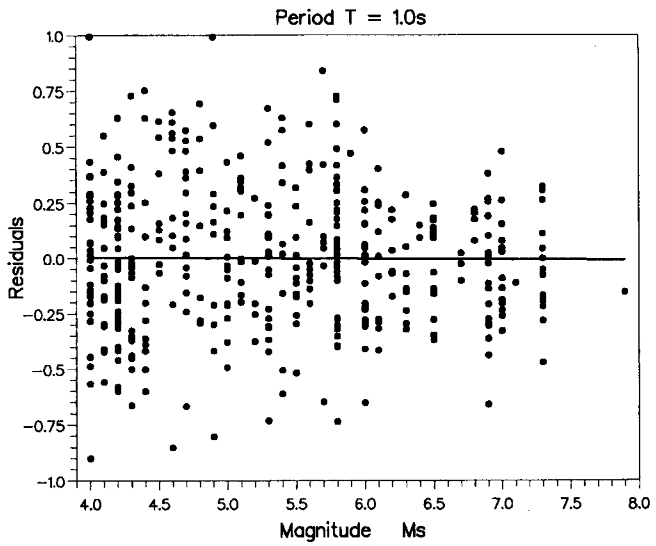

Figure 14. Residuals of the logarithm of spectral acceleration at $T = 1{\cdot}0$ s from equation (11) as a function of magnitude

It is difficult to make valid comparisons of our equations with those of Petrovski and Marcellini[5] because our definitions of source-site distance are different and they have not stated the magnitude scale used in their study, and also because they do not consider site geology. The principal difference lies in the form of their distance term $(r + C)$, where r is hypocentral distance and C is a variable term, set at 20 km for the results in their paper. This is equivalent to $[\sqrt{(d^2 + h_0^2)} + C]$ in our attenuation model, therefore to interpret any comparisons made, assumptions regarding the meaning of C are required. Their use of hypocentral distance further complicates any comparison, particularly for larger magnitude events. Figure 20 presents a spectrum form our study for a magnitude 7 event at surface fault distance of 10 km on rock. For this design situation, the hypocentral distance can vary significantly depending on the location of the site with respect to the fault plane and the choice of design focal position. Figure 20 also shows spectra of Petrovski and Marcellini[5] for epicentral distances of 10 and 30 km and focal depths of 5, 15 and 30 km, some amongst many possibilities for the given design scenario.

DISCUSSION

In current engineering practice in Europe, which is reflected in Eurocode 8, elastic design spectra are constructed by anchoring a standard response shape to an effective peak ground acceleration. Elsewhere we have reviewed the equations available for predicting peak ground acceleration in the European area.[34] In this paper we provide as an alternative, frequency-dependent attenuation relations which allow for the direct construction of hazard-consistent design spectra.

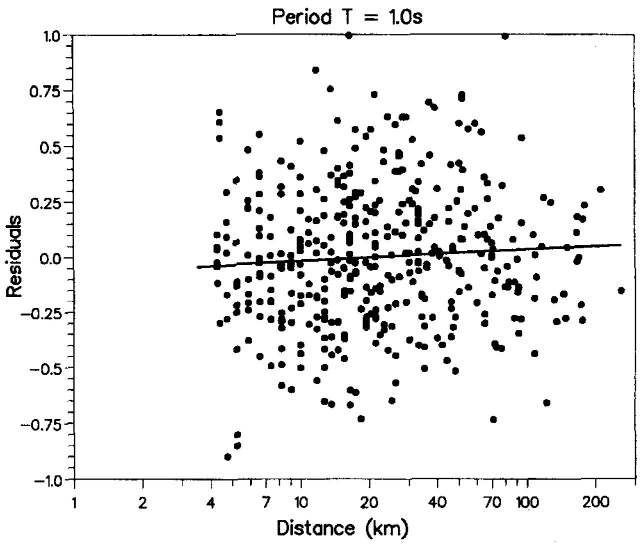

Figure 15. Residuals of the logarithm of spectral acceleration at $T = 1{\cdot}0$ s from equation (11) as a function of distance

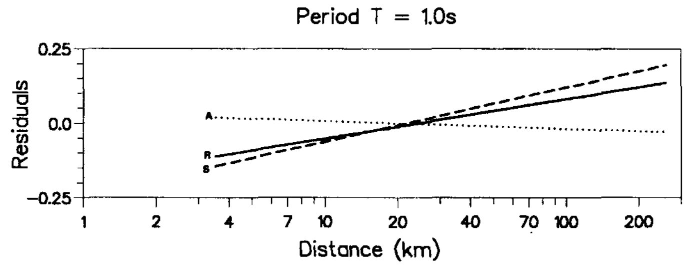

Figure 16. Regressions of residuals of logarithms of spectral acceleration at $T = 1{\cdot}0$ s, on distance for three different site categories

We have also presented equations for the prediction of peak ground acceleration based on the response spectra dataset to demonstrate that the records are representative for the region. At the same time we have explored the influence of the site geology on the amplitude of peak ground acceleration, and compared the site-dependent predictions with equations for Italy and western North America. Our equations predict larger values of peak acceleration at very short distances, particularly for larger magnitudes, but attenuate more rapidly than the equations for western North America. The differences are not very large except in the very near-field (< 5 km) of large magnitude events, a region of the curve which is sensitive to the determined h_0 value (the larger the h_0, the flatter the curve). The h_0 value itself is sensitive to the data distribution in the very near-field, which is typically sparse. The European equations do, however, show much less site-dependence, particularly for soft soil, than the equations for western North America. The Italian equations of Sabetta and Pugliese[19] predict values of acceleration which are closer to those of our European equations, although again their dependency on site geology is higher. However, it should be noted that their classification of site geology is not comparable to that used in this study. In fact, Sabetta and Pugliese[19] originally considered three site classifications, obtaining soil coefficients of 0·17 for shallow soil sites and − 0·06 for deep soil sites. Combining these two soil classes as a single group, which would be equivalent to the stiff soil (A) group in our European equations, Sabetta and Pugliese[19] found no site effect.

In order to examine the influence of the different types of site geology on the spectral response and to investigate the validity of the regression used in this study, Figure 21 shows the residuals of the logarithm of

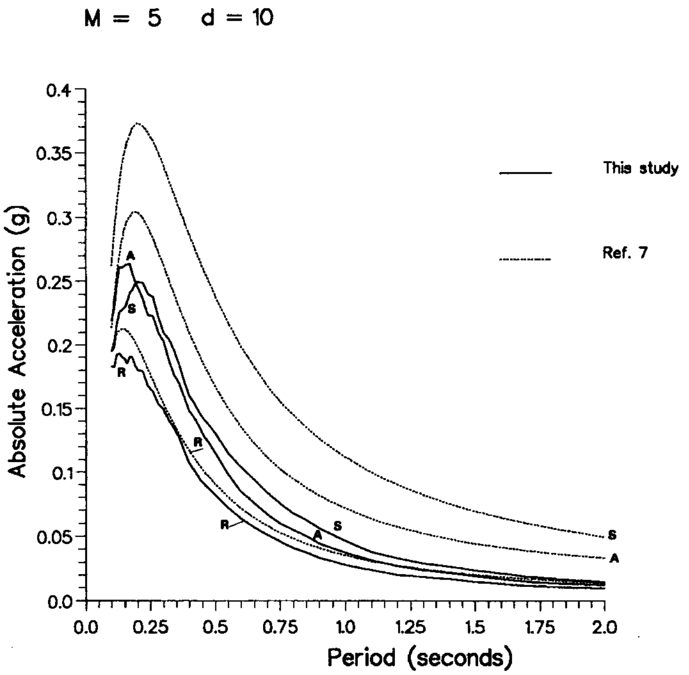

Figure 17. Absolute acceleration spectra for 5 per cent damping for rock (R), stiff soil (A) and soft soil (S) sites as predicted by this study and the equations of Boore *et al.*[7] for an earthquake of magnitude M_S 5 at a distance of 10 km

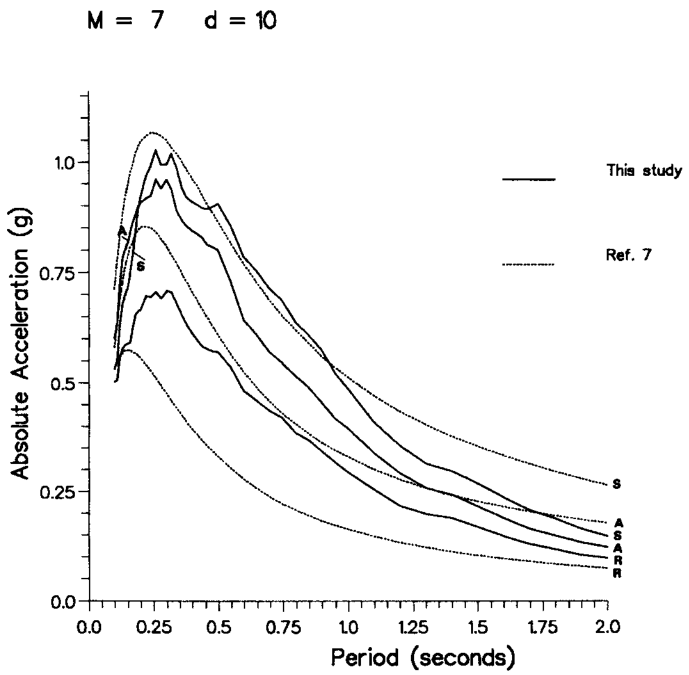

Figure 18. Absolute acceleration spectra for 5 per cent damping for rock (R), stiff soil (A) and soft soil (S) sites as predicted by this study and the equations of Boore *et al.*[7] for an earthquake of magnitude M_S 7 at a distance of 10 km

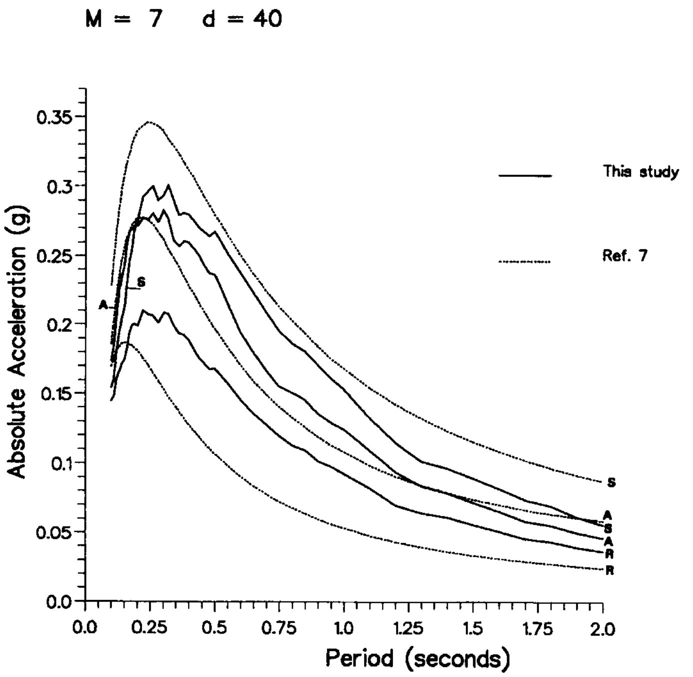

Figure 19. Absolute acceleration spectra for 5 per cent damping for rock (R), stiff soil (A) and soft soil (S) sites as predicted by this study and the equations of Boore *et al.*[7] for an earthquake of magnitude M_S 7 at a distance of 40 km

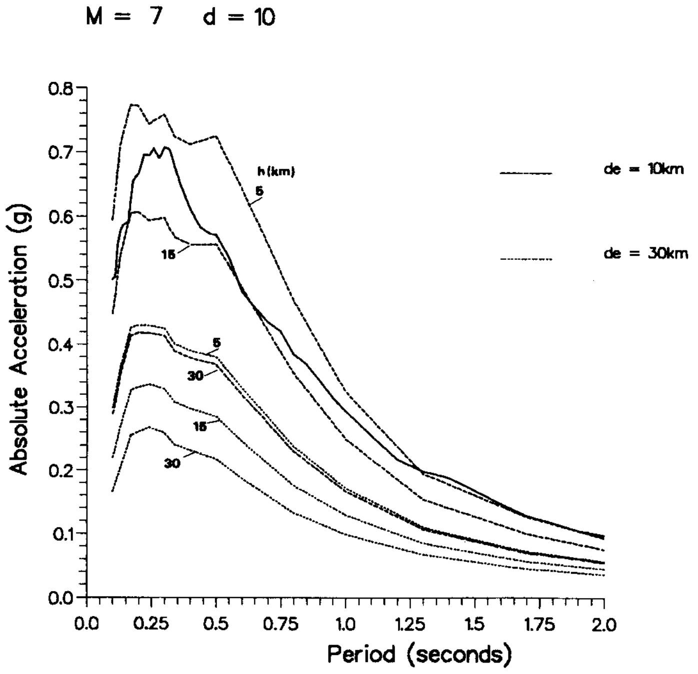

Figure 20. Response spectra (5 per cent damping) from a magnitude 7 earthquake. The solid line is the spectrum predicted by our equations for a rock site at a source distance of 10 km. The other curves correspond to predictions by Petrovski and Marcellini[5] using different focal depths and epicentral distances, as indicated

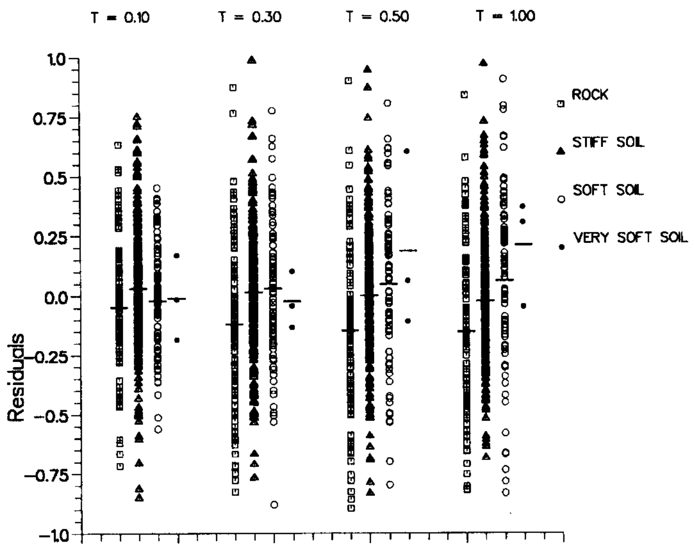

Figure 21. Residuals of the logarithm of observed spectral amplitude with respect to predicted values from equation (3) at periods of 0·1, 0·3, 0·5 and 1·0 s — independent of soil type — and grouped according to the site geology. The horizontal lines indicate the mean value of the residuals for each site grouping

the observed acceleration ordinates in our dataset with respect to the prediction using the results of the regression on distance and magnitude (equation (3)), for four different response periods. One point of interest is the amplitude of the residuals for the very soft soil (L) sites and how they compare to those from the soft soil sites (S), in order to assess the validity of their inclusion into the soft soil category. It can be seen that the three very soft points lie comfortably within the range of soft soil residuals, appearing above the soft soil mean as often as below, although clearly they tend to be above at longer periods. Repeating the regressions excluding the (L) site records resulted in a maximum change of only 4 per cent, positive or negative, in the coefficient C_S. We therefore feel there is no compelling reason to exclude these records which may well be as typical as any others.

A more important observation to be made from Figure 21 is that the differences between the mean level of the residuals for the three major site classifications is very small in comparison to the overall scatter, less than 15 per cent of the total uncertainty. Furthermore, the range and distribution of residuals are comparable in each site category. It might be expected that the soil categories, particularly soft soil, show a greater scatter of residuals due to the effects of non-linear soil behaviour. In fact the range of residuals for peak acceleration is least for soft soil and the standard deviation of the residuals about the zero mean is 0·24 for both soil groups and 0·27 for rock. This demonstrates that we should not expect to significantly increase the confidence in our predictions through the inclusion of the site geology.

It is interesting to note that many stations appear to amplify the motions from some earthquakes and de-amplify the motion in other cases, which would not be expected if the magnitude and distance were determined without error and the physical behaviour implied in our attenuation model represented the complete picture. This could suggest that there are other parameters influencing the motion that are not currently included in our model, and the site coefficients may even be functions of these parameters, as well as of magnitude and distance.

It can be seen from Figures 17–19 that, as for peak ground acceleration, the influence of site geology on the spectral amplitudes is greater for the western North American equations than for those derived for Europe, although it is comparable at larger magnitudes for stiff soil for periods less than 1·0 s and not too dissimilar for soft soil in the period range 0·3–0·9 s.

In making this comparison between the equations for Europe and western North America it is important to take into consideration that the two datasets have significantly different distributions, as can be seen

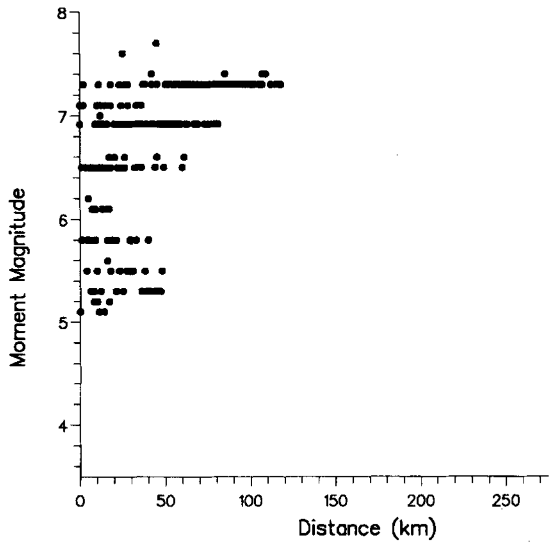

Figure 22. Distribution in magnitude and distance space of the strong-motion dataset used by Boore *et al.*[7]

comparing Figures 3 and 22. The general variation of the coefficients of our equations with increasing period are similar to those found by Boore *et al.*,[7] with the exception of the soil terms. The Boore *et al.*[7] coefficients G_B and G_C increase continually from 0·1 s, both peaking at 2·0 s. Our coefficients, C_A and C_S, vary parabolically with period, C_A peaking at shorter periods between 0·15 and 0·5 s, and C_S peaking at around 0·9 s. The trends of the other coefficients with increasing response period follow physical reasoning, for example C_4 decreases since low-frequency waves attenuate less rapidly than high-frequency waves. The variation in C_A could correspond to the fact that for a 30 m deep site with an average shear wave velocity of 550 m/s, the fundamental period would be about 0·22 s; thus peak responses would be expected at shorter periods. For category (S) sites peak responses are expected at longer periods, for example a site with 60 m of soft soil and an average shear wave velocity of 275 m/s would have a fundamental period of 0·87 s, close to the value at which C_S is highest.

It should be pointed out that the smaller values we find for the soil coefficients may in part be due to uncertainties in the site classifications, since there is considerable variation in the literature regarding the descriptions and classifications of some sites. An extreme example is the Karakyr site where the 1976 Gazli (USSR) earthquake was recorded, for which we have a shear wave velocity profile showing an average value of 151 m/s, and which has been classified as a rock site elsewhere.[20]

The maximum soil coefficients in our equations are 0·15 (T = 0·16–0·50 s) and 0·23 (T = 0·9· s) for stiff and soft soil sites, respectively, whereas for western North America these values are 0·38 and 0·55, respectively, both occurring at 2·0 s. Similarly for peak ground accelerations the additive values for the European equations are about 0·12 for both stiff and soft soil sites, whereas for western North America they are 0·16 and 0·25. The difference is unlikely to be explained only by errors in site classification because similar disagreement has been found in studies in which the actual value of V_S, which are nearly always measured values and therefore more reliable, is used as the site term in place of the dummy variables. Comparison of the equations derived in this way for Europe[31] and for western North America[8] also indicate a much higher site dependency in the latter. The influence of the site geology on the spectral response, and its interaction with the other predictor variables, is a subject of ongoing research; we find the maximum soil amplification occurring at periods of 2·0 s somewhat strange, particularly for stiff soil sites, in light of the earlier discussion of fundamental periods of different sites.

Regarding site effects, the normalized spectra of Seed *et al.*[35] have also been assessed. Seed *et al.*[35] present four curves for rock, stiff soil (< 46 m), deep cohesionless soil (> 76 m) and soft to medium clay and sand.

Table II. Comparison of additive terms to logarithm of spectral acceleration for stiff soil (A) and soft soil (S) sites compared to rock motions, from Seed *et al.*,[35] Boore *et al.*[7] and this study

	C_A			C_S		
T (s)	Reference 35	Reference 7	Equation (15)	Reference 35	Reference 7	Equation (15)
0·2	0·018	0·185	0·135	− 0·150	0·274	0·142
0·5	0·179	0·265	0·147	0·201	0·418	0·201
1·0	0·223	0·305	0·128	0·533	0·497	0·206
1·5	0·260	0·341	0·109	0·582	0·533	0·204
2·0	0·267	0·381	0·101	0·423	0·554	0·182

The curves which are comparable to ours are those for rock, stiff soil and soft to medium clay and sand, which correspond to our (R), (A) and (S) categories, respectively. The equivalent soil coefficients from the Seed *et al.*[35] study, as used in our equations, are determined by taking the logarithm of the ratio of the soil curve to the rock curve. These are given in Table II for periods 0·2, 0·5, 1·0, 1·5 and 2·0 s, together with our values and those of Boore *et al.*[7] For stiff sites, the values of Seed *et al.*[35] fall about midway between ours and those of Boore *et al.*[7] although at shorter periods (< 0·2 s) Seed *et al.*[35] show no amplification. For soft sites, the maximum amplification values of Seed *et al.*[35] are of the same order as Boore *et al.*;[7] however, these peak in the range 1·0–1·5 s, thereafter decreasing, which is similar to our curves but unlike those of Boore *et al.*,[7] which peak at 2·0 s. We also note that Seed *et al.*[35] show de-amplification on soft sites at short periods up to about 0·3 s, a feature not found by Boore *et al.*[7] or by our study.

As a final comment, we may mention the work of Pugliese and Sabetta[36] and Theodulidis and Papazachos[37] on spectral response with which we did not compare our results. The reasons for this is that one of these deals solely with a limited number of records from Italy[36] and the other with records only from Greece supplemented by data from Japan and Alaska.[37]

We are now in the process of developing predictive equations for spectral ordinates using the actual shear wave velocities as the site parameter. Also, as site-specific foundation conditions are determined for more strong-motion accelerograph stations in the European area, the equations presented herein will be modified accordingly. Whilst changes will be inevitable we do not expect to find very large differences with the current equations and we recommend the equations presented in this paper for use in engineering practice.

ACKNOWLEDGEMENTS

The authors would like to thank S. K. Sarma, M. Free and M. Srbulov for assistance in the preparation of data and for useful ideas and suggestions. The contributions of R. Berardi, B. Mohammadioun and D. Rinaldis are also gratefully acknowledged, as is the co-operation of all those individuals and agencies who contributed data. This work is supported by the European Council Environment Research Programme, contract EV5V-CT94-0490 Climatology and Natural Hazards, DG XII, Bruxelles.

APPENDIX

YR	M	D	TIME	h	M_S	DST	PHA	PHV	C	STAT	G
1969	2	28	024033	30	7·9	260	0·027	0·012	P	LISB	A
1972	1	25	202535	5	4·1	13*	0·040	0·022	I	GCIV	A
1972	1	25	232217	10	4·0	8	0·070	0·030	I	GCIV	A
1972	2	4	024218	8	4·4	2	0·125	0·078	I	GCIV	A
1972	2	4	091830	8	4·3	5	0·111	0·048	I	GCIV	A
1972	2	4	171950	2	4·2	16*	0·062	0·046	I	GCIV	A

Appendix (*contd.*)

YR	M	D	TIME	h	M_S	DST	PHA	PHV	C	STAT	G
1972	2	4	181725	10	4·0	6	0·087	0·039	I	GCIV	A
1972	2	5	012630	10	4·2	3	0·180	0·079	I	GCIV	A
1972	2	6	013419	5	4·1	2	0·225	0·087	I	GCIV	A
1972	2	8	121910	12	4·0	4	0·111	0·050	I	PALO	A
						5	0·154	0·071	I	GCIV	A
						5	0·066	0·076	I	VIGF	A
1972	6	14	185553	8	4·6	0	0·380	0·172	I	GCIV	A
						0	0·535	0·257	I	ROCC	A
						4	0·161	0·063	I	PALO	A
1972	6	14	210102	8	4·0	0	0·403	0·143	I	GCIV	A
						0	0·499	0·231	I	ROCC	A
						3	0·213	0·112	I	PALO	A
1973	11	4	155212	7	5·7	11	0·526	0·112	G	LEF1	S
1973	11	4	161136	15	4·6	14	0·075	0·023	G	LEF1	S
1973	11	23	133620	5	5·3	2	0·274	0·000	Z	MATE	A
1974	1	29	151243	13	4·1	12*	0·032	0·014	G	PAT1	A
1976	5	6	200013	6	6·5	6	0·358	0·268	I	TLM1	R
						26	0·087	0·034	I	CODR	A
						40	0·033	0·013	I	BARC	S
						69	0·073	0·024	I	CONE	A
						74	0·017	0·010	I	CORT	A
						91	0·045	0·026	I	FELT	R
						92	0·023	0·015	Y	LJB2	A
						92	0·038	0·018	Y	LJB1	R
						107	0·031	0·011	I	CASF	A
						128	0·029	0·014	I	ASIA	R
						148	0·020	0·008	I	MONS	S
						167	0·031	0·019	I	TREG	R
						177	0·038	0·019	I	MALC	A
1976	5	7	002349	8	4·8	14	0·127	0·054	I	TLM1	R
1976	5	9	005344	8	4·9	21*	0·087	0·026	I	MAI1	A
						26*	0·043	0·026	I	FORG	A
						33*	0·038	0·020	I	TLM1	R
1976	5	10	043554	5	4·2	19*	0·047	0·016	I	MAI1	A
						22*	0·030	0·014	I	FORG	A
1976	5	11	224401	12	4·7	2	0·306	0·142	I	FORG	A
						9*	0·080	0·041	I	MAI1	A
						16*	0·072	0·015	I	TARC	R
1976	5	17	025841	13	7·1	3	0·730	1·272	U	GAZL	L
1976	6	8	121438	20	4·3	31*	0·020	0·011	I	MA2T	A
						32*	0·045	0·027	I	FORG	A
1976	6	11	171636	9	4·0	5*	0·058	0·029	I	SROC	A
						6*	0·093	0·049	I	FORG	A
						12*	0·018	0·014	I	MA2T	A
						12*	0·023	0·016	I	MA2P	A
						13*	0·028	0·007	I	TLM1	R
1976	6	17	142851	15	4·2	16*	0·054	0·028	I	FORG	A
						21*	0·018	0·010	I	MA2P	A
						21*	0·020	0·013	I	MA2T	A
						27*	0·010	0·009	I	TLM1	R
1976	7	14	053934	16	4·0	17*	0·058	0·029	I	TARC	R
						26*	0·010	0·007	I	MA2T	A
						26*	0·011	0·006	I	MA2P	A
1976	8	19	011240	13	5·1	3	0·344	0·155	T	DEN1	A
1976	8	22	024915	11	4·1	15*	0·014	0·007	I	SALS	
1976	9	11	163110	6	5·5	14*	0·045	0·022	I	BUIA	S

Appendix (*contd.*)

YR	M	D	TIME	h	M_S	DST	PHA	PHV	C	STAT	G
						15	0·174	0·051	Y	BREG	A
						20*	0·070	0·018	I	SROC	A
						20*	0·110	0·050	I	FORG	A
						27	0·098	0·057	Y	KOBA	A
1976	9	11	163503	16	5·5	7	0·230	0·088	I	BUIA	S
						16	0·091	0·045	I	SROC	A
						16	0·232	0·119	I	FORG	A
						31	0·093	0·062	Y	KOBA	A
						48	0·015	0·007	I	BARC	S
						82*	0·013	0·008	I	CONE	A
						180*	0·009	0·007	I	TREG	R
1976	9	15	031519	15	6·1	9	0·110	0·076	I	BUIA	S
						12	0·122	0·058	I	SROC	A
						12	0·264	0·099	I	FORG	A
						14	0·506	0·203	Y	BREG	A
						19	0·102	0·045	Y	ROBI	R
						25	0·122	0·082	Y	KOBA	A
						35	0·030	0·014	I	CODR	A
						77	0·021	0·007	I	CONE	A
						175	0·011	0·006	I	TREG	R
1976	9	15	043854	18	4·3	9*	0·036	0·015	I	BUIA	S
						16*	0·058	0·036	I	FORG	A
						19*	0·072	0·023	Y	BREG	A
1976	9	15	092119	12	6·0	6	0·136	0·059	I	TARC	R
						7	0·421	0·132	Y	BREG	A
						8	0·091	0·091	I	BUIA	S
						9	0·235	0·083	I	SROC	A
						9	0·346	0·196	I	FORG	A
						12	0·089	0·047	Y	ROBI	R
						19	0·142	0·063	Y	KOBA	A
						35	0·025	0·010	I	BARC	S
						38	0·045	0·015	I	CODR	A
						70	0·029	0·010	I	CONE	A
						70	0·012	0·011	I	CORT	A
						88	0·022	0·009	I	FELT	R
						167	0·022	0·011	I	TREG	R
						173	0·025	0·007	I	MALC	A
1976	11	24	122216	10	7·3	44	0·098	0·054	R	MAKU	R
1977	4	6	133637	10	6·0	4	0·906	0·000	R	NAGH	A
1977	9	16	234808	15	5·2	7	0·102	0·051	I	SROC	A
						6	0·241	0·133	I	FORG	A
1977	12	9	155338	4	4·6	3	0·139	0·047	T	IZM1	S
1977	12	16	073729	4	4·9	3	0·213	0·057	T	IZM1	S
1977	12	29	165259	10	4·6	63*	0·018	0·013	G	PAT1	A
1978	3	11	192048	15	5·0	9*	0·078	0·034	I	FERR	A
						33*	0·034	0·019	I	PELL	S
1978	4	15	233348	15	5·8	11	0·162	0·050	I	PATT	L
						16	0·153	0·082	I	NASO	A
						30	0·074	0·079	I	MILA	A
						52	0·038	0·028	I	MESS	R
1978	6	20	200321	8	6·4	17	0·146	0·122	G	THES	S
1978	7	4	222328	6	5·1	15	0·115	0·053	G	THES	S
1978	9	3	050832	6	5·3	4*	0·000	0·124	G	JUNG	R
1978	9	16	153557	5	7·3	3	1·065	0·845	R	TABA	S
						11	0·389	0·172	R	DAYH	A
						34	0·105	0·075	R	BOSH	S
						94	0·103	0·055	R	FERD	S

Appendix (*contd.*)

YR	M	D	TIME	h	M_S	DST	PHA	PHV	C	STAT	G
						132	0·092	0·023	R	BAJE	A
						145	0·028	0·024	R	KHEZ	A
						166	0·027	0·015	R	SEDE	A
						170	0·018	0·016	R	BIRJ	A
						212	0·037	0·028	R	KAAS	S
1979	4	9	021021	13	5·2	14*	0·061	0·027	Y	ULC2	R
						17*	0·071	0·031	Y	ULC1	A
						30*	0·049	0·018	Y	PETR	A
1979	4	11	121426	15	4·5	19*	0·043	0·024	T	MURA	R
1979	4	15	061941	12	7·0	9	0·228	0·212	Y	ULC2	R
						9	0·292	0·459	Y	ULC1	A
						12	0·375	0·253	Y	BAR1	A
						12	0·453	0·214	Y	PETR	A
						29	0·255	0·209	Y	HERC	R
						46	0·058	0·036	Y	TGD1	R
						46	0·031	0·040	Y	TGD2	R
						65	0·074	0·026	Y	DUB1	R
						108	0·062	0·030	Y	DEBA	A
						110	0·055	0·036	Y	GACK	A
1979	4	15	063112	10	4·8*	52*	0·053	0·072	Y	ULC1	A
1979	4	15	124346	6	4·0	7*	0·060	0·024	Y	ULC1	A
1979	4	15	144306	7	5·8	22	0·093	0·045	Y	HERC	R
						24*	0·100	0·039	Y	PETR	A
						41*	0·083	0·026	Y	BAR1	A
						42*	0·054	0·030	Y	ULC1	A
1979	4	16	100440	11	4·9	1*	0·058	0·022	Y	ULC2	R
						3*	0·131	0·046	Y	ULC1	A
						21*	0·051	0·022	Y	BAR1	A
						81*	0·056	0·032	Y	HERC	R
1979	4	28	033803	15	4·2	10*	0·046	0·042	Y	BUDV	A
1979	5	10	084529	5	4·0	9	0·075	0·046	Y	BUDV	A
1979	5	12	033032	7	4·7	4	0·145	0·065	Y	BUDV	A
						20	0·086	0·033	Y	KOT1	R
1979	5	14	095307	5	4·2	7	0·038	0·018	Y	ULC2	R
						7	0·083	0·042	Y	ULC1	A
1979	5	24	172318	5	6·3	7	0·276	0·112	Y	PET2	A
						9	0·267	0·169	Y	BUDV	A
						12	0·271	0·101	Y	BAR1	A
						15	0·166	0·086	Y	TIVA	A
						18	0·077	0·044	Y	HERC	R
						19	0·057	0·034	Y	KOT2	A
						19	0·152	0·077	Y	KOT1	R
						30	0·034	0·013	Y	ULC1	A
1979	7	18	131202	5	5·0	6	0·285	0·152	T	DURS	S
1979	8	2	144148	5	4·0	16*	0·142	0·145	Y	ULC1	A
1979	9	19	213537	4	5·8	6	0·206	0·163	I	CASC	R
						21	0·088	0·053	I	ARQU	R
						21	0·042	0·042	I	SPOL	R
						33	0·039	0·023	I	BEVA	A
						37	0·038	0·011	I	MASC	A
						38	0·083	0·022	I	NOCE	A
						47*	0·022	0·011	I	VITT	R
1980	1	1	164239	5	7·0	80	0·057	0·035	Z	HORT	A
1980	6	7	183501	9	4·3	13*	0·060	0·036	I	BARG	A
						13*	0·035	0·022	I	VAGL	R
1980	10	22	162314	6	4·3	8*	0·065	0·051	A	ELSA	R
						21*	0·027	0·031	A	BENI	R

Appendix (*contd.*)

YR	M	D	TIME	h	M_S	DST	PHA	PHV	C	STAT	G
1980	10	23	095755	12	4.4	4	0.173	0.066	A	ELSA	R
						28*	0.026	0.029	A	BENI	R
1980	10	30	233813	2	4.7	17*	0.050	0.019	A	BENI	R
1980	11	8	020658	2	4.6	23*	0.028	0.022	A	BENI	R
1980	11	8	075417	8	4.9	18	0.096	0.052	A	BENI	R
1980	11	10	000148	3	4.2	24*	0.049	0.014	A	BENI	R
1980	11	23	183452	10	6.9	8	0.184	0.104	I	BAGN	R
						15	0.174	0.168	I	CALI	A
						16	0.325	0.229	I	STUR	R
						22	0.096	0.054	I	BISA	R
						23	0.060	0.036	I	AULE	R
						30	0.100	0.073	I	RION	A
						33	0.227	0.158	I	BRIE	A
						33	0.139	0.052	I	MERC	A
						41	0.055	0.028	I	BENE	A
						46	0.048	0.029	I	BOVI	S
						60	0.036	0.021	I	ARIE	R
						63	0.047	0.024	I	TRIC	A
						65	0.061	0.036	I	GREC	R
						82	0.016	0.009	I	LAUR	R
						88	0.025	0.013	I	SEVE	A
						109	0.031	0.019	I	ROCM	S
						119	0.039	0.022	I	GARI	S
						135	0.036	0.013	I	VIES	A
						48	0.018	0.011	I	GIOR	R
1980	11	24	030356	10	4.7	26	0.039	0.022	I	CALI	A
1980	11	26	145543	10	4.1	9*	0.057	0.017	I	SELV	A
						15*	0.062	0.021	I	PROC	A
1980	12	1	190431	9	4.5	5	0.084	0.045	I	OPPI	R
						5	0.080	0.025	I	PROC	A
						5	0.158	0.052	I	SELV	A
1981	1	16	003747	7	5.0	5	0.155	0.036	I	CAI1	A
						5*	0.088	0.065	I	CNZV	A
						5*	0.098	0.034	I	CNZB	A
						6	0.169	0.047	I	CAI2	A
						6*	0.072	0.033	I	CAI4	A
						4	0.153	0.053	I	CAI3	A
						8*	0.064	0.027	I	LION	R
						8*	0.108	0.025	I	PROC	A
						15*	0.021	0.014	I	CALI	A
1981	2	14	172746	10	4.5	17*	0.029	0.018	I	ARIE	R
						33*	0.014	0.012	I	GREC	R
1981	2	24	205337	10	6.7	13	0.310	0.116	G	KORI	S
						4	0.292	0.126	G	XYLO	S
1981	2	25	023551	8	6.4	24	0.118	0.045	G	KORI	S
1981	3	10	151620	10	5.3	7	0.143	0.086	G	PRE1	A
						21	0.099	0.023	G	LEF1	S
1981	4	10	083332	10	4.3	15	0.037	0.010	G	LEF1	S
1981	5	25	230400	15	4.0	7	0.057	0.021	G	LEF1	S
1981	5	27	150402	15	4.8	11	0.119	0.049	G	LEF1	S
1981	7	23	000533	20	5.6	50*	0.072	0.037	R	FARM	S
						50*	0.049	0.023	R	OROU	S
1983	1	17	124130	14	7.0	23	0.165	0.039	G	ARGO	R
						87	0.065	0.016	G	LEF3	S
						117	0.052	0.000	G	AGR1	S
1983	3	16	211941	25	4.7	16*	0.026	0.007	G	LEF3	S

Appendix (*contd.*)

YR	M	D	TIME	h	M_S	DST	PHA	PHV	C	STAT	G
1983	3	23	190402	25	4·9	26	0·051	0·014	G	LEF3	S
1983	3	23	235105	10	6·2	70	0·025	0·007	G	LEF3	S
1983	7	5	120127	7	6·0	45*	0·046	0·058	T	GONE	A
						55*	0·048	0·032	T	EDIN	R
						83*	0·026	0·017	T	EDRE	A
						95*	0·025	0·015	T	BAL1	A
1983	10	30	041228	14	6·7	17	0·166	0·060	T	HORA	A
1984	3	29	000601	15	4·1	0	0·210	0·232	T	BALI	A
1984	4	29	050259	7	5·4	16*	0·067	0·036	I	GUBB	R
						17*	0·037	0·017	I	UMBE	A
						20*	0·189	0·054	I	PIET	R
						29*	0·209	0·051	I	NOCE	A
						33*	0·052	0·015	I	CITT	S
						35*	0·009	0·008	I	CAGL	R
						50*	0·052	0·030	I	PEGL	A
1984	5	7	174943	8	5·8	12	0·110	0·065	I	ATIN	R
						17	0·147	0·096	I	CASS	A
						31*	0·069	0·026	I	PONT	R
						33*	0·087	0·032	I	ORTU	S
						39*	0·077	0·051	I	LIMA	S
						46*	0·070	0·037	I	AGAP	A
						49*	0·043	0·027	I	ROCM	S
						51*	0·024	0·009	I	BUSS	R
						52*	0·060	0·016	I	GRG1	S
						52*	0·062	0·017	I	GRG2	S
						65*	0·017	0·010	I	RIPA	A
						67*	0·029	0·017	I	CASN	A
						71*	0·012	0·014	I	BARI	S
						72*	0·017	0·008	I	POGG	A
						59*	0·132	0·075	I	MANO	R
1984	5	11	104150	8	5·3	2	0·216	0·136	I	BARR	R
						12*	0·021	0·017	I	PESC	R
						19*	0·026	0·016	I	ATIN	R
						28*	0·037	0·020	I	CASS	A
						35*	0·047	0·024	I	LIMA	S
						47*	0·027	0·014	I	AGAP	A
						55*	0·041	0·020	I	MANO	R
						17*	0·046	0·026	I	APPT	R
1984	5	11	112616	16	4·1	10*	0·024	0·011	I	APFF	R
						11*	0·022	0·028	I	BARR	R
						14*	0·029	0·024	I	PESC	R
						10*	0·016	0·009	I	APPT	R
1984	5	11	131457	12	4·3	0	0·134	0·047	I	BARR	R
						12*	0·015	0·012	I	PESC	R
						21*	0·036	0·014	I	APPT	R
						53*	0·019	0·011	I	MANO	R
1984	5	11	133902	18	4·0	6*	0·037	0·018	I	BARR	R
						13*	0·024	0·015	I	PESC	R
1984	5	11	163919	17	4·4	9*	0·024	0·007	I	APFF	R
						13*	0·035	0·026	I	BARR	R
						16*	0·017	0·014	I	PESC	R
1984	5	11	233505	8	4·4	21*	0·014	0·005	I	APPT	R
1984	6	17	074801	5	4·8	95*	0·013	0·015	T	FOC2	R
1984	8	17	212258	24	4·0	15*	0·028	0·025	G	XYLO	S
1984	10	25	094915	11	4·7	2	0·180	0·085	G	PELE	R
1985	6	12	140519	4	4·0	2	0·043	0·000	B	PROV	S

Appendix (*contd.*)

YR	M	D	TIME	h	M_S	DST	PHA	PHV	C	STAT	G
1985	8	13	134914	20	4·2	7	0·101	0·033	G	AMAL	A
1985	8	31	060347	15	4·7	13*	0·087	0·041	G	PRE1	A
						21*	0·074	0·022	G	LEF3	S
1985	12	6	223530	9	4·5	14*	0·178	0·064	T	KOYC	A
1986	5	5	033538	4	5·9	27*	0·055	0·026	T	GOLB	R
1986	6	1	064310	5	4·0	16*	0·085	0·051	T	KUSA	A
1986	6	6	103947	11	5·7	34*	0·032	0·010	T	GOLB	R
1986	9	13	172431	8	5·8	5	0·272	0·201	G	KALI	A
						5	0·297	0·330	G	KAL3	A
1986	9	15	114128	12	4·6	1*	0·240	0·104	G	KAL1	A
						1*	0·333	0·172	G	KAL3	A
						1*	0·261	0·079	G	KAL2	A
1987	5	14	062911	9	4·1	10*	0·038	0·030	G	AIG2	S
1987	10	5	092702	6	4·7	27*	0·057	0·022	G	RHOD	A
						31*	0·049	0·000	G	ARCH	R
1988	4	24	101033	5	4·2	14	0·116	0·055	G	LEF1	S
1988	5	18	051742	26	5·0	23*	0·087	0·089	G	VALS	R
1988	5	22	034415	15	4·7	11	0·080	0·035	G	VALS	R
1988	7	5	203452	10	4·8	19*	0·031	0·020	G	KORI	S
1988	9	22	120539	12	4·4	28*	0·021	0·015	G	AMAL	A
1988	10	16	123405	12	5·6	11	0·150	0·078	G	ZAKY	S
						28*	0·156	0·042	G	AMAL	A
1988	10	19	002705	10	4·0	16	0·064	0·019	G	VART	S
1988	12	7	074124	6	6·8	20	0·182	0·138	U	GUKA	S
1988	12	7	074545	11	5·8	10	0·148	0·039	U	GUKA	S
1988	12	13	110035	5	4·0	20	0·026	0·013	G	AMAL	A
1988	12	19	172936	10	4·2	3*	0·098	0·025	U	DZHR	R
						8*	0·043	0·020	U	NAL1	A
						25*	0·016	0·005	U	STP1	R
						33*	0·008	0·002	U	TOR1	A
1988	12	22	095650	10	4·1	5	0·111	0·056	G	NAFP	S
						15	0·026	0·000	G	PAT1	A
1988	12	31	040709	5	4·2	9*	0·174	0·056	U	TORI	A
						17*	0·030	0·016	U	METS	A
						18*	0·130	0·039	U	NAL1	A
						21	0·030	0·010	U	LEN1	S
						24	0·051	0·019	U	DZHR	R
						33*	0·026	0·007	U	STP1	R
1989	1	4	072941	5	4·1	11*	0·074	0·031	U	NAL1	A
						14*	0·028	0·019	U	STP1	R
						16*	0·034	0·022	U	METS	A
						34*	0·027	0·007	U	TOR1	A
1989	3	30	163624	3	4·3	14*	0·202	0·122	U	TOR1	A
1989	10	29	190913	6	5·7	9	0·289	0·135	A	CHER	S
						47	0·044	0·030	A	MEDE	A
						61	0·036	0·022	A	BOUZ	R
1990	5	17	084406	26	4·7	4	0·199	0·074	G	AIG2	S
1990	6	16	021618	29	5·3	39*	0·035	0·015	G	PRE1	A
1990	6	20	210008	19	7·3	51	0·187	0·096	R	QAZV	A
						65	0·094	0·085	R	RUDS	S
						67	0·213	0·077	R	ABHA	S
						78	0·135	0·036	R	TONE	S
						151	0·106	0·042	R	GACH	R
						183	0·014	0·028	R	TEHR	
						183	0·032	0·017	R	SARI	
1990	8	8	003507	10	4·2	15*	0·022	0·017	G	KAL3	A

Appendix (*contd.*)

YR	M	D	TIME	h	M_S	DST	PHA	PHV	C	STAT	G
						35*	0·037	0·012	G	SPAR	S
1990	12	16	154551	28	5·1#	15*	0·041	0·058	U	BOGD	A
						21*	0·118	0·068	U	BAVR	A
						19*	0·033	0·012	U	AKHA	R
						51*	0·067	0·023	U	TOR2	R
						65*	0·007	0·010	U	LEN2	S
						44*	0·042	0·012	U	BAKU	R
						70*	0·023	0·009	U	STP2	A
						72*	0·013	0·011	U	KARA	A
						91*	0·007	0·004	U	KIRO	A
1990	12	21	065743	13	6·1	31	0·102	0·041	G	EDES	L
						49*	0·050	0·030	G	KILK	A
1990	12	23	212851	5	4·1#	73*	0·011	0·005	U	STP2	A
1991	04	29	091248	6	6·9	108	0·011	0·006	U	AKHA	R
						122	0·009	0·006	U	BOGD	A
1991	05	03	201939	6	5·3#	9*	0·508	0·136	U	AMBR	A
						24*	0·052	0·016	U	ONIB	A
						24*	0·078	0·036	U	ONI	A
						34*	0·025	0·014	U	IRI	A
1991	05	03	234101	6	4·4#	12*	0·049	0·022	U	ONI	A
						12*	0·035	0·011	U	ONIB	A
						13*	0·205	0·054	U	AMBR	A
						22*	0·019	0·011	U	IRI	A
1991	05	10	012515	4	4·0#	7*	0·040	0·022	U	AMBR	A
						11*	0·066	0·019	U	ZEMO	A
						32*	0·013	0·007	U	SACH	
1991	05	10	203043	8	4·2#	7*	0·078	0·014	U	ONIB	A
						11*	0·052	0·034	U	IRI	A
						9*	0·028	0·015	U	ZEMO	A
						18*	0·012	0·007	U	SACH	
						21*	0·007	0·003	U	AMBR	A
1991	05	15	142849	6	4·2#	4*	0·166	0·113	U	ZEMO	A
						7*	0·066	0.016	U	ONIB	A
						8*	0·056	0·022	U	ONI	A
						17*	0·043	0·020	U	IRI	A
						16*	0·049	0·008	U	AMBR	A
1991	06	15	005920	6	6·2	39*	0·112	0·043	U	IRI	A
						50*	0·036	0·015	U	ONIB	A
						50*	0·072	0·016	U	ONI	A
						59*	0·061	0·025	U	ZEMO	A
						71*	0·017	0·007	U	AMBR	A
1992	3	13	171840	10	6·8	4	0·504	0·242	T	ERZN	A
						67*	0·030	0·017	T	TERC	A
						75*	0·071	0·036	T	REFA	A
1992	3	15	161625	10	5·8	45*	0·106	0·055	T	ERZN	A
						45*	0·039	0·018	T	ERZS	A
1992	5	30	185540	12	4·8	33	0·027	0·026	G	AMAL	A
						37	0·068	0·021	G	PAT1	A
1992	11	6	190809	17	6·0	30*	0·039	0·021	T	IZM2	A
						40*	0·081	0·063	T	KUSA	A
						60*	0·029	0·014	T	CESM	
1992	11	18	211941	15	5·7	25*	0·038	0·026	G	AIG2	S
						36*	0·022	0·018	G	MRN1	R
1993	2	4	022259	5	4·7	9*	0·100	0·099	G	XYLO	S
1993	3	26	114515	10	4·3	0*	0·196	0·054	G	PYRG	S
						15*	0·056	0·024	G	AMAL	A

Appendix (*contd.*)

YR	M	D	TIME	h	M_S	DST	PHA	PHV	C	STAT	G
1993	3	26	115613	10	4·3	6*	0·124	0·057	G	PYRG	S
						11*	0·048	0·036	G	AMAL	A
1993	3	26	115815	10	5·3	4*	0·434	0·121	G	PYRG	S
						19*	0·114	0·058	G	AMAL	A
1993	3	26	124913	10	4·0*	14	0·067	0·020	G	AMAL	A
1993	6	13	232640	15	5·1	37*	0·019	0·012	G	PRE1	A
						33	0·146	0·087	G	LEF1	S
1993	7	10	202604	10	4·2	13	0·076	0·026	G	AMAL	A
1993	7	14	123149	15	5·6	5*	0·401	0·124	G	PAT3	A
						8*	0·188	0·070	G	PAT1	A
						8*	0·175	0·048	G	PAT2	S
						25*	0·050	0·037	G	NAFP	S
						29*	0·052	0·027	G	AIG2	S
						36*	0·031	0·020	G	MESO	S
						55*	0·026	0·010	G	AMAL	A
1993	9	26	075326	10	4·2	15*	0·061	0·014	G	ZAK2	S
1993	11	4	051837	10	5·3	10*	0·104	0·052	G	NAFP	S
						18*	0·028	0·021	G	AIG2	S
						19*	0·014	0·011	G	PAT1	A
1994	1	14	060748	10	4·5*	19*	0·088	0·021	G	ZAK2	S
1994	2	25	023051	10	5·4	16*	0·200	0·058	G	LEF1	S
						29*	0·035	0·018	G	PRE1	A
1994	2	27	223452	10	4·1*	27*	0·083	0·033	G	LEF1	S

Notes: The table headings arae as follows: YR—year; M—month; D—day; TIME—origin time in UTC; h—focal depth in km; M_S—surface wave magnitude; DST—distance from source to station (as defined in text) in km; PHA, PHV—peak horizontal and vertical accelerations, in g; C—country or region where record obtained; STAT—code of strong-motion station; G—soil conditions at the site classified on the basis of the average shear wave velocity over the upper 30 m: R > 750 m/s, A 360–750 m/s, S 180–360 m/s and L < 180 m/s. Country codes are: A—Algeria, B—Bulgaria, I—Italy, G—Greece, P—Portugal, R—Iran, T—Turkey, U—former USSR, Y—former Yugoslavia, Z—Azores. M_S values marked by an asterix have been converted from M_L values via empirical relations derived for the European area[38] and those marked by # have been converted from energy scale K values reported by agencies in the former Soviet Union. Distances marked by an asterix are epicentral.

REFERENCES

1. R. K. McGuire, 'Seismic design spectra and mapping procedures using hazard analysis based directly on oscillator response', *Earthquake eng. struct. dyn.* **5**, 211–234 (1977).
2. R. A. Johnson, 'An earthquake spectrum prediction technique', *Bull. seism. soc. Am.* **63**, 1255–1274 (1973).
3. W. B. Joyner and D. M. Boore, 'Prediction of earthquake response spectra', *Open-File Report. 82-977*, United States Geological Survey, 1982.
4. C. B. Crouse, K. V. Yogesh and B. A. Schell, 'Ground motions from subduction-zone earthquakes', *Bull. seism. soc. Am.* **78**, 1–25, (1988).
5. D. Petrovski and A. Marcellini 'Prediction of seismic movement of a site: statistical approach', *Proc., UN sem. on predict. of earthquake*, Lisbon, 14–18 November 1988.
6. A. Dahle, H. Bungum and L. B. Kvamme, 'Attenuation models inferred from intraplate earthquake recordings', *Earthquake eng. struct. dyn.* **19**, 1125–1141 (1991).
7. D. M. Boore, W. B. Joyner and T. E. Fumal, 'Estimation of response spectra and peak accelerations from western North American earthquakes: an interim report', *Open-File Report 93-509*, United States Geological Survey, 1993.
8. D. M. Boore, W. B. Joyner and T. E. Fumal, 'Estimation of response spectra and peak accelerations from western North American earthquakes: an interim report, Part 2', *Open-File Report 94-127*, United States Geological Survey, 1994.
9. I. M. Idriss, 'Characteristics of earthquake ground motion', *Proc., ASCE speciality conf. soil dyn. earthquake eng.*, Pasadena, vol. III, 1151–1265, 1978.
10. N. M. Newmark and W. J. Hall, 'Seismic design criteria for nuclear reactor facilities', *Proc. 4th world conf. earthquake. eng.*, Vol. II, Santiago, 1969, pp. B5.1–B5.12.
11. N. M. Newmark, J. A. Blume and K. K. Kapur, 'Seismic design spectra for nuclear power plants', *J. power div. ASCE* **99**, 287–303 (1973).
12. K. Kawashima, K. Aizawa and K. Takahashi, 'Attenuation of peak ground motion and absolute acceleration response spectra', *Proc. 8th world conf. earthquake eng.* Vol. II, San Francisco, 1984, pp. 257–264.

13. W. B. Joyner and D. M. Boore, 'Measurement, characterization and prediction of strong ground motion', *Proc. earthquake eng. soil dyn. II, ASCE GT div.*, Park City, Utah, 1988, pp. 43-102.
14. B. Mohammadioun, 'The prediction of response spectra for the anti-seismic design of structures specificity of data from intracontinental environments', *Eur. earthquake eng.* **5**, 8–17 (1991).
15. N. N. Ambraseys and J. J. Bommer, 'Database of European strong ground-motion records', *Eur. earthquake eng.* **5**, 18–37 (1991).
16. J. J. Bommer and N. N. Ambraseys, 'An earthquake strong-motion databank and database', *Proc. 10th world conf. earthquake eng.*, Vol. I, Madrid, 1992, pp. 207–210.
17. W. B. Joyner and D. M. Boore, 'Peak horizontal acceleration and velocity from strong-motion records including records from the 1979 Imperial Valley, California, earthquake', *Bull. seism. soc. Am.* **71**, 2011–2038 (1981).
18. K. W. Campbell, 'Near source attenuation of peak horizontal acceleration', *Bull. seism. soc. Am.* **71**, 2039–2070 (1981).
19. F. Sabetta and A. Pugliese, 'Attenuation of peak horizontal acceleration and velocity from Italian strong-motion records', *Bull. seism. soc. Am.* **77**, 1491–1513 (1987).
20. N. A. Abrahamson and J. J. Litehiser, 'Attenuation of vertical peak acceleration', *Bull. seism. soc. Am.* **79**, 549–580 (1989).
21. J. Vanek, A. Zapotek, V. Karnik, V. Kondorskaya, E. F. Riznichenko, S. L. Solv'ev and N. V. Shebalin 'Standardization of magnitude scales', *Izvestiya acid. nauk SSSR, ser. geofiz.* **2**, 153–158 (1962).
22. V. Karnik, *Seismicity of the European area: Part I*. D. Reidel, Dordrecht, Holland, 1969.
23. T. C. Hanks and H. Kanamori, 'A moment magnitude scale', *J. geophys. res.* **84**, 2348–2350 (1979).
24. H. Kanamori, 'The energy release in great earthquakes', *J. geophys. res.* **82**, 2981–2987 (1977).
25. G. Ekström and A. M. Dziewonski, 'Evidence of bias in estimation of earthquake size', *Nature* **332**, 319–323, (1988).
26. SHWP, 'A review of seismotectonics of Britain in the context of NW Europe' *Report on seismic hazard assessment'*, Vol. 3J, Seismic Hazard Working Party, Nuclear Electric, 1993.
27. R. J. Scherer and G. I. Schüeller, 'Records and power spectra of corrected and integrated strong motion earthquake data', Vol. I: *Friuli earthquake sequence of 1976*. Part A: overview and theoretical background of data processing, Innsbruck-Munich, 1985.
28. J. M. H. Menu, 'Engineering study of near-field earthquake strong-motions', *Ph.D. thesis*, University of London, 1986.
29. S. Shyam Sunder and J. Connor, 'A new procedure for processing strong-motion earthquake signals', *Bull. seism. soc. Am.* **72**, 643–661 (1982).
30. N. N. Ambraseys and J. J. Bommer, 'The attenuation of ground accelerations in Europe', *Earthquake eng. struct. dyn.* **20**, 1179–1202 (1991).
31. N. N. Ambraseys, 'The prediction of earthquake peak ground acceleration in Europe', *Earthquake eng. struct. dyn.* **24**, 467–490 (1995).
32. S. K. Sarma, 'Fortran program ATTEN', *ESEE Internal Report*, Imperial College, London, 1994.
33. CIT, 'Analyses of strong motion earthquake accelerograms - response spectra. Vol. III, Part A', *Report No. EERL 72-70*, Earthquake Engineering Research Laboratory, California Institute of Technology, Pasadena, 1973.
34. N. N. Ambraseys and J. J. Bommer, 'Attenuation relations for use in Europe: an overview', *SECED conf. Eur. seis. design practice*, Chester, 1995, pp. 67–74.
35. H. B. Seed, C. Ugas and J. Lysmer, 'Site-dependent spectra for earthquake resistant design', *Report No. EERC 74-12*, Earthquake Engineering Research Center, University of California, Berkeley, 1974.
36. A. Pugliese and F. Sabetta, 'Stima di spettri di riposta da registrazioni di forti terremoti italiani', *Ingegneria sismica* **VI**, 3–14 (1989).
37. N. P. Theodulidis and B. C. Papazachos, 'Dependence of strong ground motion on magnitude-distance, site geology and macroseismic intensity for shallow earthquakes in Greece: II, horizontal pseudovelocity', *Soil dyn. earthquake eng.* **13**, 317–343 (1994).
38. N. N. Ambraseys and M. W. Free, 'Surface wave magnitude calibration for European region earthquakes', ESEE Internal Report, Imperial College, London, 1995.